UC Davis
UC Davis Previously Published Works

Title

Hyperglycemia regulates cardiac K+ channels via O-GlcNAc-CaMKII and NOX2-ROS-PKC pathways

Permalink

https://escholarship.org/uc/item/4x95j2v1

Journal

Basic Research in Cardiology, 115(6)

ISSN

0300-8428

Authors

Hegyi, Bence
Borst, Johanna M
Bailey, Logan RJ
et al.

Publication Date

2020-12-01

DOI

10.1007/s00395-020-00834-8

Peer reviewed

Hyperglycemia regulates cardiac K+ channels via *O*-GlcNAc-CaMKII and NOX2-ROS-PKC pathways

Bence Hegyi[1], **Johanna M. Borst**[1], **Logan R. J. Bailey**[1], **Erin Y. Shen**[1], **Austen J. Lucena**[1], **Manuel F. Navedo**[1], **Julie Bossuyt**[1], **Donald M. Bers**[1]

[1]Department of Pharmacology, University of California Davis, 451 Health Sciences Drive, Davis, CA, USA

Abstract

Chronic hyperglycemia and diabetes lead to impaired cardiac repolarization, K^+ channel remodeling and increased arrhythmia risk. However, the exact signaling mechanism by which diabetic hyperglycemia regulates cardiac K^+ channels remains elusive. Here, we show that acute hyperglycemia increases inward rectifier K^+ current (I_{K1}), but reduces the amplitude and inactivation recovery time of the transient outward K^+ current (I_{to}) in mouse, rat, and rabbit myocytes. These changes were all critically dependent on intracellular *O*-GlcNAcylation. Additionally, I_{K1} amplitude and I_{to} recovery effects (but not I_{to} amplitude) were prevented by the Ca^{2+}/calmodulin-dependent kinase II (CaMKII) inhibitor autocamtide-2-related inhibitory peptide, CaMKIIδ-knockout, and *O*-GlcNAc-resistant CaMKIIδ-S280A knock-in. I_{to} reduction was prevented by inhibition of protein kinase C (PKC) and NADPH oxidase 2 (NOX2)-derived reactive oxygen species (ROS). In mouse models of chronic diabetes (streptozotocin, *db*/*db*, and high-fat diet), heart failure, and CaMKIIδ overexpression, both I_{to} and I_{K1} were reduced in line with the downregulated K^+ channel expression. However, I_{K1} downregulation in diabetes was markedly attenuated in CaMKIIδ-S280A. We conclude that acute hyperglycemia enhances I_{K1} and I_{to} recovery via CaMKIIδ-S280 *O*-GlcNAcylation, but reduces I_{to} amplitude via a NOX2-ROS-PKC pathway. Moreover, chronic hyperglycemia during diabetes and CaMKII activation downregulate K^+ channel expression and function, which may further increase arrhythmia susceptibility.

Keywords

Potassium channels; CaMKII; ROS; Hyperglycemia; Diabetes

Introduction

Diabetes mellitus (DM) and its hallmark metabolic abnormality, hyperglycemia, are closely associated with cardiovascular morbidity and mortality [9]. While the best characterized cardiac complications of DM include coronary artery disease and structural remodeling of the heart, DM is also associated with increased cardiac arrhythmia risk [18]. Among electrophysiological derangements that promote arrhythmias, altered K^+ channel function leads to impaired action potential repolarization and is considered an important contributor to arrhythmogenesis [36, 40]. Critically, previous studies have reported downregulation of cardiac K^+ channel expression and decreased K^+ currents in animal models of both type 1 and type 2 DM (T1DM and T2DM, respectively) [22, 27, 29, 35, 39, 51, 54]. However, the signaling pathways by which diabetic hyperglycemia regulates K^+ channels in the heart are unknown.

Calcium/calmodulin-dependent kinase II (CaMKII) is upregulated in diabetes and contributes to both cardiac remodeling and arrhythmias [11, 15, 21, 25]. Hyperglycemia has been shown to induce posttranslational modification of CaMKII by O-linked β-N-acetylglucosamine (O-GlcNAc) on Serine 280, inducing autonomous kinase activity [11]. In line with this, inhibition of either CaMKII or O-GlcNAcylation prevented spontaneous diastolic Ca^{2+} leak and arrhythmias in diabetic hyperglycemia [11]. CaMKII is also known to regulate K^+ channels acutely by phosphorylation of the channel proteins and chronically by altering their expression [48]. However, the contribution of CaMKII to K^+ channel remodeling during hyperglycemia and diabetes has not been investigated.

Oxidative stress is also frequently implicated in the pathophysiology of DM [13]. Multiple mechanisms can lead to increased generation of reactive oxygen species (ROS) in diabetic hyperglycemia, including enhanced NADPH oxidase 2 (NOX2) activity and a variety of derangements in mitochondrial metabolism [13, 24]. ROS regulates diverse cellular mechanisms, including excitation–contraction coupling, transcription, inflammation, and cell death [5]. ROS can also modulate ion channels either through direct protein modification or through oxidative stress-dependent activation of protein kinases, including protein kinase C (PKC) [12] and CaMKII [10]. However, the exact signaling mechanism of ROS-dependent K^+ channel regulation are unclear. Therefore, mechanistic understanding of how diabetic hyperglycemia regulates K^+ channels will be essential to understanding the mechanisms of arrhythmogenesis and designing more effective antiarrhythmic therapies in DM. We aimed to investigate the changes in major cardiac voltage-gated K^+ currents during acute hyperglycemia and diabetes. We hypothesized that hyperglycemia regulates K^+ channel biophysics and expression by activating CaMKII via O-GlcNAcylation and/or oxidation.

Methods

Animal models

Several types of adult male C57BL/6 J mice (10–12 weeks) were used, including wild-type (WT, Jackson Laboratory, Stock No. 000664), CaMKIIδ-knockout (KO) [23], CaMKIIδ$_C$ (predominant cytosolic isoform)-overexpression (OE) [53], oxidation-resistant CaMKIIδ-

MM281/282VV [25], and *O*-GlcNAc-resistant CaMKIIδ-S280A knock-in [24], and NOX2-knockout (Jackson Laboratory, Stock No. 002365). For rat and rabbit experiments, adult male Wistar rats (10–14 weeks) and New Zealand White rabbits (3–4 months) were used.

Isolation of left ventricular cardiomyocytes was performed as previously described [14]. Briefly, animals were injected with heparin (5000 U/kg) and anesthetized with isoflurane (5%). Hearts were excised and retrograde perfused on constant flow Langendorff apparatus (5 min, 37 °C) with Ca^{2+}-free normal Tyrode's solution, gassed with 100% O_2. Then, ventricular myocytes were digested using Liberase TM (0.225 mg/mL, Roche) for mice and rats, and collagenase type II (Worthington) and protease type XIV (Sigma-Aldrich) for rabbits. Ventricular myocytes were dispersed mechanically and filtered through a nylon mesh then allowed to sediment for 10 min. The sedimentation was repeated three times using increasing $[Ca^{2+}]$ from 0.125 to 0.25 then 0.5 mmol/L. Finally, ventricular myocytes were kept in Tyrode's solution [0.5 mmol/L (Ca^{2+})] at room temperature until use.

DM was studied in three different mouse models: streptozotocin (STZ)-induced T1DM [21, 35], high-fat diet (HFD)-induced T2DM [32, 43] and *db/db*, a genetic model of T2DM (leptin-receptor deficiency) [2, 20]. In the first model, diabetes was induced in 6–8-week-old mice by intra-peritoneal injections with low-dose STZ (50 mg/kg body weight in 40 mmol/L sodium citrate, pH = 4.0) for 5 consecutive days and littermates received sodium citrate as vehicle control. Only mice exhibiting > 300 mg/dL blood glucose levels for 4 weeks following STZ injections (≈ 70% success rate) were included in the study. In the second model, mice were fed with HFD (60 kcal% fat, D12492, Research Diets) starting at 5 weeks of age for 16 weeks, whereas controls received low-fat diet (LFD, 10 kcal% fat, D12450J, Research Diets). In the third model, 10-week-old *db/db* mice (Jackson Laboratory, Stock No. 000642) were used and wild-type C57BLKS/J mice (Jackson Laboratory, Stock No. 000662) served as control. Blood glucose levels were assessed using OneTouch UltraMini (LifeScan) glucose monitoring system and test strips.

Transverse aortic constriction (TAC) with a 28G stenosis was performed in 8-week-old mice to induce pressure overload which led to heart failure (HF) in 8 weeks following the surgery. A sham procedure without banding the thoracic aorta was performed in control animals.

Electrophysiology

Isolated cardiomyocytes were transferred to a temperature-controlled chamber (Warner Instruments) mounted on a Leica DMI3000 B inverted microscope, and continuously perfused with Tyrode solution containing (in mmo/L): NaCl 140, KCl 4, $CaCl_2$ 1.8, $MgCl_2$ 1, HEPES 5, Na-HEPES 5, glucose 5.5 and mannitol 24.5; pH = 7.40 and osmolality = 320 ± 2 mOsm/L. High glucose effects were assessed 6-min following bath medium switch to a Tyrode solution containing 30 mmol/L glucose and 0 mannitol (osmolality and pH matched). Electrodes were fabricated from borosilicate glass (World Precision Instruments) having tip resistances of 2–2.5 MΩ when filled with internal solution containing (in mmol/L): K-Aspartate 100, KCl 20, NaCl 8, Mg-ATP 5, EGTA 10, $CaCl_2$ 4.1, HEPES 10, cAMP 0.002, phosphocreatine-K_2 10, and calmodulin 0.0001, with pH = 7.2 free $[Ca^{2+}]_i$ = 100 nmol/L, calculated using the Web Maxc Extended version of MaxChelator software (https://somapp.ucdmc.ucdavis.edu/pharmacology/bers/maxchelator/webmaxc/

webmaxcE.htm). The electrodes were connected to the input of an Axopatch 200B amplifier (Axon Instruments). Outputs from the amplifier were digitized at 50 kHz using Digidata 1332A A/D card (Axon Instruments) under software control (pClamp 10). The series resistance was typically 3–5 MΩ and it was compensated by 90%. Experiments were discarded when the series resistance was high or increased by > 10%. Reported voltages are already corrected for liquid junction potentials.

Whole-cell K^+ currents were recorded in the presence of Na^+ and Ca^{2+} current inhibitors (10 μmol/L tetrodotoxin and 10 μmol/L nifedipine) in the bath solution. Different K^+ current components were separated using appropriate voltage protocols and selective ionic channel inhibitors. The rapidly inactivating transient outward K^+ current (I_{to}) and slowly inactivating K^+ current ($I_{K,slow}$) in mouse were distinguished by biexponential fits ($R^2 > 0.9$ in each case) of the time-dependent decay of K^+ current that is sensitive to 3 mmol/L 4-aminopyridine (4-AP) or by sensitivity of $I_{K,slow}$ to 50 μmol/L 4-AP, as previously described [3, 50]. The non-inactivating steady-state K^+ current (I_{SS}) in mouse was the 4-AP insensitive residual K^+ current. The rapid delayed rectifier K^+ current (I_{Kr}) and the inward rectifier K^+ current (I_{K1}) were sensitive to 1 μmol/L E-4031 and 300 μmol/L Ba^{2+}, respectively. Ionic currents were normalized to cell capacitance, determined in each cell using short (10 ms) hyperpolarizing pulses from – 10 mV to – 20 mV. All experiments were conducted at 37 ± 0.1 °C.

Detailed description of the voltage protocols and drug treatments are provided in the Supplemental Methods.

Transcript analysis using qRT-PCR

Total RNA from 8- to 10-week-old male CaMKIIδ knockout, overexpression, S280A and WT littermate ($N = 3$ each), and 16-week-old (8-week post-surgery) TAC and sham WT ($N = 3$ each) mouse hearts was extracted using RNeasy Mini Kit (Qiagen). Conversion to cDNA was performed using QuantiTect Reverse Transcription Kit (Qiagen). Transcript analysis of genes encoding CaMKIIδ (*Camk2d*), CaMKIIγ (*Camk2g*), markers of cardiomyocyte hypertrophy (β-myosin heavy chain, *Myh7*; atrial natriuretic factor, *Anf*), K^+ channel pore forming and auxiliary subunits, as well as housekeeping control genes, including glyceraldehyde 3-phosphate dehydrogenase (*Gapdh*) and *S18* ribosomal protein was carried out using quantitative real-time polymerase chain reaction (qRT-PCR) on an Applied Biosystems 7900HT Fast Real-Time PCR System and Primer–Probe detection. Three technical replicates were performed for each biological sample. The primers were from Eurofins Genomics and their sequences are provided in Suppl. Table 1. Transcript data were normalized to the arithmetic mean of *Gapdh* and *S18*, and analysed using the threshold cycle (C_T) relative quantification method, then linearized ($2^{- C_T}$) to make comparison.

Western blot analysis of $K_{ir}2.1$ protein expression

Hearts from WT, CaMKIIδ-KO, CaMKIIδ-OE and CaMKIIδ-S280A mice ($N = 3$ each) were collected and lysed in ice-cold buffer containing (in mmol/L): NaCl 150, HEPES (pH = 7.5) 10, NaF 50, sodium pyrophosphate 1, $MgCl_2$ 1, EGTA 1, EDTA 1, 1% Triton X-100, and protease and phosphatase inhibitors (EMD Millipore, set III and V, respectively). Protein

concentration was determined by BCA assay (cat#23225, Thermo Fisher Scientific). Sample proteins were then separated by SDS-PAGE (4–20%) before transferring to a 0.2 μm nitrocellulose membrane. Immunoblots were blocked with 8% milk in 0.05% TBS-Triton (TBST). The blots were then incubated overnight at 4 °C with primary antibodies for $K_{ir}2.1$ (NeuroMab, Cat#: 75–210, Lot#: 455-6JD.13, 1:1000) and GAPDH (Abcam, Cat#: ab181602, Lot#: GR199633-12, 1:10,000). Following five TBST washes, specific secondary antibodies were applied for 2 h at room temperature. The blots were again washed sequentially in TBST, TBS and water before imaging on the Sapphire Biomolecular Imager (Azure Biosystem). Three blots were made for each protein sample.

Echocardiography

Transthoracic echocardiography was performed in anesthetized (isoflurane, 0.5–2%) animals before and after STZ and TAC procedures. Short axis M-mode images of the left ventricles were acquired using a Vevo 2100 echocardiography system (FUJIFILM VisualSonics, Toronto, ON, Canada) equipped with a 40 MHz transducer. Body temperature was carefully monitored, and anesthesia was adjusted to achieve ≈ 450 beats/min heart rate in each animal.

Statistics

Data are presented as mean ± SEM. The number of cells/animals (n/N) in each experimental group was reported in the figures. Statistical significance was tested using paired, two-tailed Student's t test or two-way ANOVA followed by a post-hoc Bonferroni or Tukey test when applicable. Graph-Pad Prism 8.0 and Origin 2016 software were used. A p value of less than 0.05 was considered significant.

Results

Acute hyperglycemia affects the function of K^+ channels in mouse ventricular myocytes

First, we tested the effect of high glucose (30 mmol/L) corresponding to what is observed in severe diabetes versus osmotically-matched (glucose substituted with equimolar mannitol) low glucose (5.5 mmol/L) on major voltage-gated K^+ channels in mouse ventricular myocytes at 37 °C (Fig. 1a, b). Acute hyperglycemia (6 min) significantly reduced I_{to}, whereas $I_{K,slow}$ and I_{SS} were unchanged (Fig. 1c-e). The fast and slow inactivation kinetics of I_{to} were unaltered in hyperglycemia (Fig. 1f). However, the recovery from inactivation kinetics of I_{to} were significantly enhanced by 20–26% in hyperglycemia (Fig. 1g). Importantly, I_{K1} was increased in hyperglycemia (Fig. 1h, paired data obtained in individual cells are shown in Suppl. Fig.1a). I_{Kr} was small in mice and unaltered by acute hyperglycemia (Suppl. Fig.1b).

Hyperglycemia effects on K^+ channels are shared between species

K^+ channel expression in the heart is significantly different between species [40]. Therefore, we also tested the effects of hyperglycemia in rat and rabbit ventricular myocytes (which more closely resemble human cardiomyocyte electrophysiology). Although basal I_{to} density was smaller (I_{to}: rabbit < rat < mouse) and no $I_{K,slow}$ was observed in rat and rabbit myocytes, hyperglycemia induced similar I_{to} reduction in both species (Fig. 2a, b). However, I_{to} recovery from inactivation was faster in rat vs. mouse (Fig. 2c). In rabbit, roughly half of

total I_{to} exhibited very slow recovery kinetics (often distinguished as $I_{to,slow}$ vs. $I_{to,fast}$; Fig. 2d). Importantly, hyperglycemia enhanced I_{to} recovery in both species (Fig. 2c, d). In contrast to I_{to}, basal I_{K1} density was larger in rat and rabbit myocytes compared to mouse (I_{K1}: mouse < rat < rabbit) and acute hyperglycemia further increased I_{K1} in both species (Fig. 2e, f). These data demonstrate that the effects of acute hyperglycemia on K^+ channels are similar across 3 species.

O-GlcNAc modifications mediate the effects of hyperglycemia on K⁺ channels

Impairment of the hexosamine biosynthetic pathway (HBP) leading to enhanced *O*-GlcNAcylation has been implicated in diabetic arrhythmias [11]. Therefore, we examined the contribution of *O*-GlcNAc modifications to K^+ channel regulation in hyperglycemia in mouse (Fig. 3a). HBP and its end-product UDP-GlcNAc are necessary for *O*-GlcNAc protein modifications. This pathway can be inhibited using the broad spectrum amidotransferase inhibitor 6-diazo-5-oxo-L-norleucine (DON) and the selective *O*-GlcNAc transferase (OGT) inhibitor OSMI-1. Strikingly, pretreatment with either DON or OSMI-1 prevented all acute hyperglycemia effects on K^+ channels and had no effect in normoglycemia (Fig. 3b-f). Conversely, when *O*-GlcNAc removal by *O*-GlcNAc*ase* (OGA) was inhibited using Thiamet-G (Thm-G, 6 min), the same K^+ channel effects observed under hyperglycemia were also observed under normoglycemic conditions (Fig. 3b-f). These data suggest that *O*-GlcNAcylation is necessary and sufficient for the observed hyperglycemia-induced K^+ channel regulation.

Glucose dose–response effects and the impact of extracellular K⁺ concentration on I_K1

Next, we measured I_{K1} in rabbit myocytes acutely exposed to increasing concentrations of glucose (osmolarity was matched using mannitol). I_{K1} magnitudes in 5.5 mmol/L and 10 mmol/L glucose were indistinguishable, whereas 20 mmol/L glucose induced a nonsignificant trend towards increased I_{K1}, and 30 mmol/L glucose was sufficient to induce a significant increase in I_{K1} (Fig. 4a, b). When we repeated the experiments in the presence of insulin (5 nmol/L) to increase glucose uptake in cardiomyocytes via GLUT4 [42], this only slightly promoted glucose effects on I_{K1} (Fig. 4b). However, Thm-G markedly enhanced glucose effects on I_{K1} (Fig. 4b). These data suggest that in healthy control myocytes, hyperglycemia can affect K^+ channels in a graded manner which can be further shifted by enhanced glucose uptake or perturbation of the HBP (e.g., here by Thm-G). Indeed, the balance between addition and removal of *O*-GlcNAc is regulated through OGT and OGA, respectively, which may be impaired in DM [26].

I_{K1} is also critically regulated by the level of extracellular K^+, and it is known that both hypo- and hyperkalemia may frequently occur in diabetic patients [9]. Hypo- and hyperkalemia not only shifted the reversal potential (E_K) of I_{K1}, but also markedly altered I_{K1} amplitude and the voltage, where outward I_{K1} peaked (Fig. 4c, d). Hyperglycemia did not alter the measured E_K or V_m for peak outward I_{K1} (Fig. 4d) but similarly increased I_{K1} in both hyper- and hypokalemia (Fig. 4e, f).

CaMKII and PKC mediate the effects of hyperglycemia on K$^+$ channels

We tested the contribution of protein kinases which may mediate the downstream effects of hyperglycemia and could be regulated by O-GlcNAc modifications (Fig. 5a). Cells were pretreated (for 15 min) with specific kinase inhibitors, including autocamtide-2-related inhibitory peptide (AIP), protein kinase inhibitor peptide (PKI), and bisindolylmaleimide II (BIM-II) to selectively inhibit CaMKII, protein kinase A (PKA), and PKC, respectively. AIP and PKI pre-incubations used myristoylated forms and the peptides were also included in pipette solution to optimize inhibition. At baseline, these inhibitors had no effect on K$^+$ channels except for CaMKII inhibition using AIP, which slightly reduced I_{K1} (Fig. 5b, c). However, AIP prevented the hyperglycemia effects on I_{K1} and I_{to} recovery, but not on the reduction of I_{to} amplitude (Fig. 5b-f). PKI did not affect any of the measured K$^+$ currents in hyperglycemia (Fig. 5b-f). Interestingly, the hyperglycemia-induced decrease in I_{to} amplitude was prevented only by the PKC inhibitor BIM-II (Fig. 5d). We further examined the involvement of PKC in regulating I_{to} using Go 6976 that selectively inhibits the Ca^{2+}-dependent conventional PKC isoforms (PKCα and PKCβ; Fig. 5g). Cell pretreatment with Go 6976 did not change baseline I_{to} but prevented the hyperglycemia-induced reduction of I_{to} amplitude (Fig. 5h, i). Because PKC inhibitor staurosporine and derivates thereof may directly inhibit K$^+$ channels (off-target effect) [45], we also used BIM-V, a structurally related but inactive analogue of these PKC inhibitors. BIM-V did not change I_{to} amplitude and did not prevent I_{to} reduction in hyperglycemia (Fig. 5h, i).

NOX2-dependent ROS production mediates the effects of hyperglycemia on I_{to}

Increased production of ROS via NOX2 and mitochondrial mechanisms has been implicated in diabetic hyperglycemia [13]. Because ROS is known to regulate both CaMKII (by oxidizing 2 neighboring methionines, MM281/282) [10] and PKC [8], we tested the involvement of ROS in regulating K$^+$ channels in acute hyperglycemia (Fig. 6a). Pretreatment of the cells with ROS scavengers L-glutathione (GSH) and N-acetylcysteine (NAC) slightly reduced baseline I_{K1} but did not alter the hyperglycemia-induced I_{K1} increase (Fig. 6b, c). This same lack of ROS scavenger effect was also true for the accelerated kinetics of I_{to} recovery (Fig. 6e, f), but ROS scavengers abolished the hyperglycemia-induced I_{to} amplitude reduction (Fig. 6d). NOX2-KO also abolished the effect of hyperglycemia on I_{to} amplitude, but not on I_{K1} amplitude or I_{to} recovery kinetics (Fig. 6b-f). Oxidation-resistant CaMKIIδ-MM281/2VV knock-in showed normal baseline K$^+$ channel phenotype and all acute hyperglycemia effects on K$^+$ channels were present (Fig. 6b-s). These functional fingerprints in Figs. 5 and 6 indicate that acute hyperglycemia reduces I_{to} amplitude via a NOX2-ROS-PKC pathway, but that CaMKII mediates the I_{K1} and I_{to} recovery effects, which are independent of ROS and CaMKII oxidation.

CaMKIIδ-S280 O-GlcNAcylation mediates hyperglycemia effects on I_{to} recovery and I_{K1}

We further investigated the effects of hyperglycemia in myocytes isolated from CaMKIIδ-KO, CaMKIIδ-OE, and O-GlcNAc-resistant CaMKIIδ-S280A mice. First, we tested the baseline K$^+$ currents measured in normoglycemia in each CaMKII genotype to assess CaMKII-dependent chronic regulation (i.e., functional expression), then acute hyperglycemic effects therein to assess acute regulation (Fig. 7a).

CaMKIIδ-KO exhibited substantially larger amplitudes of I_{to}, $I_{K,slow}$ and I_{SS}, faster I_{to} inactivation, and faster I_{to} recovery from inactivation *vs.* WT (Fig. 7b-g). Conversely, CaMKIIδ-OE reduced I_{to} and I_{SS} but enhanced the slow component of I_{to} recovery *vs.* WT, whereas $I_{K,slow}$ and I_{to} inactivation were unchanged (Fig. 7b-g). I_{K1} was slightly increased in CaMKIIδ-KO and markedly reduced in CaMKIIδ-OE (Fig. 7h, i). The small I_{Kr} in mouse was further reduced in CaMKIIδ-OE (Fig. 6J). Most of these baseline effects are consistent with the expected directions of effect for chronic inhibition or enhancement of CaMKII [48]. Importantly, all K^+ currents were unchanged in CaMKIIδ-S280A at baseline (note dashed horizontal lines for WT control; Fig. 7a-j).

Acute hyperglycemia reduced I_{to} amplitude in all CaMKIIδ genotypes (Fig. 7b), in line with the data obtained using CaMKII inhibitor AIP (Fig. 5d), and that CaMKII is not involved in acute reduction of I_{to} amplitude. However, the acute hyperglycemia effects on I_{to} recovery (Fig. 7f, g) and I_{K1} amplitude (Fig. 7h, i) were prevented in CaMKIIδ-KO, confirming the AIP data (Fig. 5b, c) and CaMKIIδ involvement. Importantly, these CaMKII-mediated hyperglycemia effects were also prevented in CaMKIIδ-S280A (Fig. 7f-i) indicating the critical role of CaMKIIδ-S280 *O*-GlcNAcylation in autonomously activating CaMKII in hyperglycemia. Moreover, the hyperglycemia-induced reduction in I_{to} amplitude that seemed CaMKII-independent above, was almost identical in the CaMKIIδ-S280A mouse to that observed in WT mice (Fig. 7b). Thus, the mediation of these hyperglycemia-induced changes in I_{to} and I_{K1} seems very consistent with respect to molecular mechanism, involving either *O*-GlcNAcylation at CaMKIIδ-S280 and CaMKII-dependent phosphorylation (I_{K1} and I_{to} recovery kinetics) and *O*-GlcNAc-dependent activation of NOX2 and PKC-dependent phosphorylation (I_{to} amplitude reduction).

Chronic CaMKII activation downregulates K⁺ channel expression

Because chronic CaMKII activation led to hypertrophic cardiac remodeling and changes the functional expression of K^+ channels (Fig. 7), we examined which genes were responsible for the K^+ current remodeling. Using qRT-PCR we found markedly increased expression of hypertrophic genes (*Anf, Myh7*) in CaMKIIδ-OE (having ~ 50-fold higher *Camk2d* transcript level, Fig. 8a and Suppl. Fig.2). In CaMKIIδ-OE, several K^+ channel genes were downregulated, including *Kcnd2, Kcnd3, Kcnip2, Kcna5, Kcnk3, Kcnj2, Kcnh2a, Kcnh2b*, and *Kcnq1*, whereas *Kcne1* was upregulated (Fig. 8b). Interestingly, some of these K^+ channel genes were reciprocally regulated in CaMKIIδ-KO, including upregulation of *Kcnd3, Kcnb1* and *Kcnk3*, and downregulation of *Kcne1* (Fig. 8b). However, the expression of *Kcnd2, Kcnip2, Kcna5, Kcnh2a, Kcnh2b* and *Kcnq1* was unchanged in CaMKIIδ-KO (Fig. 8b). No change in the expression of any genes was found in CaMKIIδ-S280A (Fig. 8b), in line with its normal baseline phenotype (Fig. 8a). The protein expression profile of $K_{ir}2.1$ (predominant I_{K1} channel isoform) closely followed its gene (*Kcnj2*) expression level with marked reduction in CaMKIIδ-OE, a nonsignificant increasing trend in CaMKIIδ-KO, and no change in CaMKIIδ-S280A (Fig. 8c). These expression data are in line with the K^+ current densities in CaMKIIδ mutants. Moreover, these data provide insights on which K^+ channels are responsible for the observed differences in K^+ current densities in CaMKIIδ-KO and CaMKIIδ-OE (Fig. 7).

K+ channel functional expression and regulation in chronic diabetes

Next, we measured K^+ currents in three diabetic animal models (Fig. 9a) including STZ-induced T1DM *vs.* vehicle-injected controls [21, 35], HFD-induced T2DM *vs.* LFD [32, 43], and *db/db vs.* WT C57BLKS/J [2, 20], see "Animal models" in "Methods" for details. Diabetic animals exhibited increased blood glucose levels and moderate cardiomyocyte hypertrophy (Suppl. Fig. 3a, b). The K^+ channel remodeling was studied in an early phase of the disease (e.g., 4-week post-STZ) with preserved cardiac systolic contractile function (no change in fractional shortening and ventricular diameters) as measured by echocardiogram (Suppl. Table 2).

Importantly, all K^+ currents, including I_{to}, $I_{K,slow}$, I_{SS}, I_{K1} and I_{Kr}, were already reduced in all three diabetic models in this early, cardiac-compensated phase of DM. The largest reduction in K^+ currents was found in the STZ model (Fig. 9b-g), similar to that observed in CaMKIIδ-OE (Fig. 7). STZ mice showed no change in I_{to} inactivation kinetics and only a slight enhancement of I_{to} slow recovery (Suppl. Fig. 3c-e). However, in STZ myocytes acute hyperglycemia (as occur in vivo in these diabetic animals) induced a further reduction in I_{to} (Fig. 9b), but increased I_{K1} (Fig. 9e, f) and further enhanced I_{to} recovery (Suppl. Fig. 3d, e). This recapitulates the situation that there is still dynamic hyperglycemic modulation of channel properties that rides on top of changes in expression in the STZ model. Surprisingly, cardiomyocytes from HFD and *db/db* were resistant to the effects of acute hyperglycemia on both I_{to} amplitude and recovery, and I_{K1} magnitude (Fig. 9b, e, f, and Suppl. Fig. 3d, e).

Next, we tested whether CaMKIIδ-S280A is also protective against chronic hyperglycemia effects. Due to limited number of animals available and parallel uses of cells in different studies, we focused on the decreased I_{K1} density, because it was the most pronounced alteration in DM. Importantly, I_{K1} reduction was markedly attenuated in STZ-treated CaMKIIδ-S280A (Fig. 9h, i). In individual cells, the membrane capacitance (an indirect measure of cell size) was correlated with decreasing I_{K1} density in STZ-treated WT, but this relationship was absent in WT control and STZ-treated CaMKIIδ-S280A (Fig. 9j). This data suggests that CaMKIIδ-S280 *O*-GlcNAcylation in DM is responsible for mediating both hypertrophic and I_{K1} functional effects at a single cell level.

K+ channel functional expression and hyperglycemic response in heart failure

HF is a frequent comorbidity in diabetic patients, and diabetes increases the risk of newly developing HF [9]. CaMKII is also upregulated in HF and contributes to maladaptive cardiac remodeling and arrhythmias [23]. We, therefore, tested the effect of hyperglycemia in a mouse model of HF. We used the well-established TAC model in mice to induce cardiac hypertrophy and HF. 8-week post-surgery mice exhibited 45% decrease in fractional shortening, 30% increase in systolic ventricular diameter, 70% increase in heart weight/body weight ratio, and pulmonary edema (Suppl. Table 3). The voltage-gated K^+ currents were all significantly decreased in TAC *vs.* sham (Fig. 10a-c), similar to that seen in CaMKIIδ-OE (Fig. 7) and DM (Fig. 9). The expression of the K^+ channels was also downregulated in TAC-induced HF (Fig. 10d) in accordance with the changes in K^+ currents. The K^+ channel expression profile in TAC (in which *Camk2d* was twofold upregulated) largely overlapped with that of CaMKIIδ-OE. However, a few differences existed, including *Kcna4* and *Kcne1*

downregulation in TAC mice (Fig. 10d) vs. their upregulation in CaMKIIδ-OE mice (Fig. 8c). This suggests additional CaMKIIδ-independent K^+ channel regulatory mechanisms in HF. Moreover, acute hyperglycemia further reduced I_{to}, but enhanced its recovery and increased the markedly decreased I_{K1} in TAC (Fig. 10a-c).

Discussion

The increased arrhythmia risk and the lack of effective antiarrhythmic therapies in DM highlight the need for a better understanding of the molecular underpinnings of arrhythmogenesis in this disease. The pathophysiology of DM is undisputedly complex, but K^+ channel remodeling is strongly implicated as a main driver of arrhythmogenicity [15]. K^+ channel downregulation contributes to action potential and QT prolongation frequently observed in patients with DM [4], enhancing arrhythmogenic substrate in the heart. Moreover, due to the increased membrane resistance when I_{K1} is reduced, a given inward current can cause larger depolarizations, promoting triggered activities [34]. Previous reports in line with our data here (Fig. 9) showed decreases in several K^+ currents in DM, including I_{to}, $I_{K,slow}$, I_{K1}, I_{Kr}, and I_{Ks} in accordance with the reduced expression of $K_V4.2$ (*Kcnd2*), $K_V4.3$ (*Kcnd3*), KChIP2 (*Kcnip2*), $K_V1.5$ (*Kcna5*), $K_{ir}2.1$ (*Kcnj2*), hERG/$K_V11.1$ (*Kcnh2*), and $K_V7.1$/minK (*Kcnq1*/*Kcne1*), respectively [22, 27, 29, 35, 39, 51, 54].

Acute hyperglycemia may also increase arrhythmia risk [15]. In healthy human volunteers, hyperglycemic-clamp to 15 mmol/L plasma glucose for 2 h slightly prolonged QTc interval (from 413 to 442 ms) and markedly increased QTc dispersion (from 32 to 55 ms) independent of insulin action [28]. Clinical data in diabetic patients also demonstrates that postprandial hyperglycemia and glucose-variability are independent risk factors of cardiovascular disease [6]. Moreover, patients with T2DM had a slightly higher risk of ventricular premature beats during their hyperglycemic vs. normoglycemic periods [7]. Furthermore, hyperglycemia is also strongly associated with increased risk of early-onset ventricular tachycardia following myocardial infarction both in diabetic and non-diabetic patients [46]. However, the underlying molecular mechanisms for promoting arrhythmias in either chronic or acute hyperglycemia are still incompletely understood.

Acute hyperglycemia regulates K^+ currents via *O*-GlcNAcylation and CaMKII and PKC

Existing work on the mechanisms of acute hyperglycemic alteration of K^+ channels is sparse and focused only on ATP-sensitive K^+ channels in cardiomyocytes [19] and large-conductance Ca^{2+}-activated K^+ channels in arterial smooth muscle cells [32]. Here, in three species, we found that acute hyperglycemia significantly altered I_{to} and I_{K1} in ventricular cardiomyocytes, which are known to critically influence AP morphology and arrhythmias. However, the acute reduction in I_{to} amplitude observed may be partially compensated by enhanced I_{to} recovery kinetics at higher heart rates. Moreover, the increased I_{K1} observed may provide some protection against hyperglycemia-induced diastolic Ca^{2+} leak and afterdepolarizations, another characteristic consequence of CaMKII activation [11, 15]. However, changes in $[K^+]_o$ (Fig. 4) and chronic remodeling in K^+ channels in DM (Fig. 9) and HF (Fig. 10) may shift the relative K^+ channel balance (mostly downregulation) to promote arrhythmias.

Signaling mechanisms contributing to K^+ channel regulation in acute and chronic hyperglycemia are poorly characterized, but crucial for potential therapeutic targeting in DM. We found that the hyperglycemic effects on both I_{to} and I_{K1} were mediated by the HBP and in particular via O-GlcNAcylation (Figs. 1, 2, 3). Furthermore, two separate pathways mediated these effects: I_{to} downregulation was dependent on the NOX2-ROS-PKC signaling axis (Figs. 5, 6), while the enhanced I_{to} recovery and I_{K1} amplitude were dependent entirely on activation of CaMKIIδ by S280 O-GlcNAcylation (Fig. 7). Moreover, the acute CaMKII-dependent enhancement of I_{K1} amplitude and I_{to} recovery were maintained in CaMKIIδ-OE, T1DM and HF, and in altered $[K^+]_o$ (for I_{K1}) and mimicked simply by inhibition of O-GlcNAc*ase*. However, these acute hyperglycemic effects were abolished by inhibition of CaMKII or O-GlcNAc transferase and in CaMKIIδ-KO, -S280A mutant and T2DM (both HFD and *db/db*, Fig. 9). The underlying mechanism for this loss of acute hyperglycemic I_{K1} enhancement in T2DM is unclear, but may include altered glucose uptake, insulin signaling and cell metabolism, or differential baseline protein O-GlcNAcylation [26].

Environmental factors such as hyperglycemia and oxidative stress can lead to posttranslational modifications and play an important role in the pathophysiology of DM [13, 26]. O-GlcNAcylation was demonstrated previously to activate CaMKIIδ [11] and O-GlcNAc modifications may also regulate PKCα, yet the level of O-GlcNAc-modified PKCα correlated negatively with its activity [37]. Nevertheless, oxidative stress activates both CaMKII [10] and PKC [12]. Moreover, both CaMKII [24, 31] and PKC [17] may further induce NOX2 and increase ROS production, thus forming a vicious positive feedback cycle in DM-induced progression of cardiac dysfunction.

Prior works on PKC and CaMKII-dependent regulation of K^+ channels are in line with our data (Fig. 5). PKC activation was found to reduce I_{to} in adult rat cardiomyocytes and both $K_V4.2$ and $K_V4.3$ currents expressed in Xenopus oocytes without significant changes in channel biophysics [30]. PKC was further shown to phosphorylate the C-terminus (T503) of the long isoform of $K_V4.3$ (but not the short splice variant), and reduce I_{to} in human cardiomyocytes [33]. We found that this PKC-mediated I_{to} reduction in diabetic hyperglycemia was critically dependent on oxidative stress (Fig. 6) in agreement with an earlier report [51]. CaMKII, on the other hand, was previously demonstrated to enhance I_{to} recovery [48] by phosphorylating $K_V4.3$ at S550 [41] and $K_V1.4$ at S123 [38], suggesting a mechanistic basis for hyperglycemia-induced enhancement of both the fast ($K_V4.2/4.3$) and slow ($K_V1.4$) components of I_{to} recovery seen in Figs. 1, 2. Acute I_{K1} enhancement by CaMKII activation (Figs. 1, 2, 3) was also previously reported [16, 48]; however, the exact phosphorylation site of CaMKII on $K_{ir}2.1$ has not yet been identified. CaMKII may also acutely increase the slow delayed rectifier K^+ current (I_{Ks}) [16], the ATP-sensitive K^+ current [52] and the Ca^{2+}-activated K^+ current [44]. The regulation of these channels in hyperglycemia requires further studies.

Chronic K^+ channel expression and current reduction with CaMKIIδ, DM and HF

K^+ channel remodeling during T1DM and T2DM development in mouse models (Fig. 9) resembled that seen in CaMKIIδ-OE (Figs. 7, 8) and HF (Fig. 10), which is consistent with CaMKII involvement in the regulation of K^+ channel expression in DM at the level of gene

expression/transcription. We show direct evidence for this mechanism in that the decrease in I_{K1} following STZ-induced T1DM was markedly attenuated in CaMKIIδ-S280A (Fig. 9). We also demonstrated a correlation between I_{K1} reduction and increasing cell capacitance in individual cells following STZ treatment (Fig. 9). This relationship was abolished in STZ-treated CaMKIIδ-S280A mice, suggesting that CaMKII O-GlcNAcylation initiates myocyte transcriptional remodeling and expression of a hypertrophic gene program [53]. This hypothesis should be explored in future studies.

Upon chronic activation, both PKC [47] and CaMKII [49] phosphorylate class II histone deacetylases (HDACs) which lead to their nuclear export and altered gene transcription. Accordingly, CaMKIIδ-OE was shown here (Fig. 8) and previously [48] to decrease I_{K1} and I_{to}, in line with the downregulation of mRNA and protein levels of $K_V4.2$ (*Kcnd2*), $K_V4.3$ (*Kcnd3*), KChIP2 (K*cnip2*) and $K_{ir}2.1$ (*Kcnj2*). CaMKIIδ-OE also downregulated $I_{K,slow}$, I_{SS} and I_{Kr} in line with the decreased expression of *Kcna5*, *Kcnk3* and *Kcnh2a/2b*. Expression of I_{Ks} channel mRNAs were also altered in CaMKIIδ-OE with reduction of the pore-forming *Kcnq1* subunit and an increase in the β subunit *Kcne1* (Fig. 8). Interestingly, reduced *Kcne1* expression mediated by the Ca^{2+}/calcineurin/NFAT axis has been described following sustained β-adrenergic stimulation [1]. In line with this finding, in TAC-induced HF we observed a tendency for reduced *Kcne1* expression (Fig. 10).

The present study has advanced fundamental understanding of the mechanisms of both acute and chronic K^+ channel alterations in hyperglycemia and diabetes. The broad downregulation of K^+ channels in both DM and HF and the role of CaMKII paints a picture of reduced repolarization reserve that may contribute similarly to increased arrhythmogenic propensity in both pathologies. Due to altered myocyte glucose metabolism in HF, enhanced CaMKII O-GlcNAcylation has also been observed in the hearts of non-diabetic HF patients, and even higher levels of O-GlcNAcylated CaMKII has been observed in HF patients with DM [11]. Moreover, CaMKII O-GlcNAcylation has also been shown in brain samples of diabetic patients [11] and may occur in other organs as well. Overall, these data highlight the need for future studies to characterize the role of CaMKII O-GlcNAcylation in the pathogenesis of both cardiac and other systemic complications of DM.

Conclusions

We found that O-GlcNAcylation of CaMKII at S280 enhanced I_{K1} and I_{to} recovery from inactivation during acute hyperglycemia. However, chronic CaMKII activation in diabetes and HF significantly downregulated the functional expression of most K^+ channels. Additionally, a NOX2-ROS-PKC pathway significantly decreased I_{to} amplitude in hyperglycemia. These data suggest that while acute hyperglycemia effects on K^+ channels may be compensated for in a healthy heart, chronic hyperglycemia and CaMKII activation can cause significant arrhythmogenic electrophysiological remodeling. Thus, a better understanding of mechanisms of K^+ channel regulation in diabetic hyperglycemia may elucidate specific downstream targets amenable to precision medicine interventions, enabling design of better antiarrhythmic therapeutics in DM.

Data availability

All data and materials are available on reasonable request to the corresponding author.

Supplementary Material

Refer to Web version on PubMed Central for supplementary material.

Acknowledgements

Abbreviations

4-AP	4-Aminopyridine
AIP	Autocamtide-2-related inhibitory peptide
ANF	Atrial natriuretic factor
BIM	Bisindolylmaleimide
CaMKII	Ca^{2+}/calmodulin-dependent kinase II
DM	Diabetes mellitus
DON	6-Diazo-5-oxo-L-norleucine
HBP	Hexosamine biosynthetic pathway
HF	Heart failure
HFD	High-fat diet
I_{Kr}	Rapid delayed rectifier K^+ current
I_{Ks}	Slow delayed rectifier K^+ current
I_{Kslow}	Slowly inactivating K^+ current
I_{K1}	Inward rectifier K^+ current
I_{SS}	Steady-state K^+ current
I_{to}	Transient outward K^+ current
LFD	Low-fat diet

NOX2	NADPH oxidase 2
Myh7	β-Myosin heavy chain
OE	Overexpression
***O*-GlcNAc**	*O*-Linked β-*N*-acetylglucosamine
OGA	*O*-GlcNAc*ase*
OGT	O-GlcNAc transferase
PKI	Protein kinase inhibitor
PKC	Protein kinase C
ROS	Reactive oxygen species
STZ	Streptozotocin
TAC	Transverse aortic constriction
Thm-G	Thiamet-G
T1DM	Type 1 diabetes mellitus
T2DM	Type 2 diabetes mellitus

References

1. Aflaki M, Qi XY, Xiao L, Ordog B, Tadevosyan A, Luo X, Maguy A, Shi Y, Tardif JC, Nattel S (2014) Exchange protein directly activated by cAMP mediates slow delayed-rectifier current remodeling by sustained beta-adrenergic activation in guinea pig hearts. Circ Res 114:993–1003. 10.1161/CIRCRESAHA.113.302982 [PubMed: 24508724]

2. Boudina S, Abel ED (2007) Diabetic cardiomyopathy revisited. Circulation 115:3213–3223. 10.1161/CIRCULATIONAHA.106.679597 [PubMed: 17592090]

3. Brouillette J, Clark RB, Giles WR, Fiset C (2004) Functional properties of K^+ currents in adult mouse ventricular myocytes. J Physiol 559:777–798. 10.1113/jphysiol.2004.063446 [PubMed: 15272047]

4. Brown DW, Giles WH, Greenlund KJ, Valdez R, Croft JB (2001) Impaired fasting glucose, diabetes mellitus, and cardiovascular disease risk factors are associated with prolonged QTc duration. Results from the Third National Health and Nutrition Examination Survey. J Cardiovasc Risk 8:227–233. 10.1177/174182670100800407 [PubMed: 11551001]

5. Burgoyne JR, Mongue-Din H, Eaton P, Shah AM (2012) Redox signaling in cardiac physiology and pathology. Circ Res 111:1091–1106. 10.1161/CIRCRESAHA.111.255216 [PubMed: 23023511]

6. Ceriello A (2005) Postprandial hyperglycemia and diabetes complications: is it time to treat? Diabetes 54:1–7. 10.2337/diabetes.54.1.1 [PubMed: 15616004]

7. Chow E, Bernjak A, Williams S, Fawdry RA, Hibbert S, Freeman J, Sheridan PJ, Heller SR (2014) Risk of cardiac arrhythmias during hypoglycemia in patients with type 2 diabetes and cardiovascular risk. Diabetes 63:1738–1747. 10.2337/db13-0468 [PubMed: 24757202]

8. Cosentino-Gomes D, Rocco-Machado N, Meyer-Fernandes JR (2012) Cell signaling through protein kinase C oxidation and activation. Int J Mol Sci 13:10697–10721. 10.3390/ijms130910697 [PubMed: 23109817]

9. Cosentino F, Grant PJ, Aboyans V, Bailey CJ, Ceriello A, Delgado V, Federici M, Filippatos G, Grobbee DE, Hansen TB, Huikuri HV, Johansson I, Juni P, Lettino M, Marx N, Mellbin LG,

Ostgren CJ, Rocca B, Roffi M, Sattar N, Seferovic PM, Sousa-Uva M, Valensi P, Wheeler DC, Group ESCSD (2020) 2019 ESC Guidelines on diabetes, pre-diabetes, and cardiovascular diseases developed in collaboration with the EASD. Eur Heart J 41:255–323. 10.1093/eurheartj/ehz486 [PubMed: 31497854]

10. Erickson JR, Joiner ML, Guan X, Kutschke W, Yang J, Oddis CV, Bartlett RK, Lowe JS, O'Donnell SE, Aykin-Burns N, Zimmerman MC, Zimmerman K, Ham AJ, Weiss RM, Spitz DR, Shea MA, Colbran RJ, Mohler PJ, Anderson ME (2008) A dynamic pathway for calcium-independent activation of CaMKII by methionine oxidation. Cell 133:462–474. 10.1016/j.cell.2008.02.048 [PubMed: 18455987]

11. Erickson JR, Pereira L, Wang L, Han G, Ferguson A, Dao K, Copeland RJ, Despa F, Hart GW, Ripplinger CM, Bers DM (2013) Diabetic hyperglycaemia activates CaMKII and arrhythmias by O-linked glycosylation. Nature 502:372–376. 10.1038/nature12537 [PubMed: 24077098]

12. Geraldes P, King GL (2010) Activation of protein kinase C isoforms and its impact on diabetic complications. Circ Res 106:1319–1331. 10.1161/CIRCRESAHA.110.217117 [PubMed: 20431074]

13. Giacco F, Brownlee M (2010) Oxidative stress and diabetic complications. Circ Res 107:1058–1070. 10.1161/CIRCRESAHA.110.223545 [PubMed: 21030723]

14. Hegyi B, Banyasz T, Izu LT, Belardinelli L, Bers DM, Chen-Izu Y (2018) beta-adrenergic regulation of late Na$^+$ current during cardiac action potential is mediated by both PKA and CaMKII. J Mol Cell Cardiol 123:168–179. 10.1016/j.yjmcc.2018.09.006 [PubMed: 30240676]

15. Hegyi B, Bers DM, Bossuyt J (2019) CaMKII signaling in heart diseases: emerging role in diabetic cardiomyopathy. J Mol Cell Cardiol 127:246–259. 10.1016/j.yjmcc.2019.01.001 [PubMed: 30633874]

16. Hegyi B, Bossuyt J, Ginsburg KS, Mendoza LM, Talken L, Ferrier WT, Pogwizd SM, Izu LT, Chen-Izu Y, Bers DM (2018) Altered repolarization reserve in failing rabbit ventricular myocytes: calcium and beta-adrenergic effects on delayed- and inward-rectifier potassium currents. Circ Arrhythm Electrophysiol 11:e005852. 10.1161/CIRCEP.117.005852 [PubMed: 29437761]

17. Inoguchi T, Li P, Umeda F, Yu HY, Kakimoto M, Imamura M, Aoki T, Etoh T, Hashimoto T, Naruse M, Sano H, Utsumi H, Nawata H (2000) High glucose level and free fatty acid stimulate reactive oxygen species production through protein kinase C–dependent activation of NAD(P)H oxidase in cultured vascular cells. Diabetes 49:1939–1945. 10.2337/diabetes.49.11.1939 [PubMed: 11078463]

18. Jouven X, Lemaitre RN, Rea TD, Sotoodehnia N, Empana JP, Siscovick DS (2005) Diabetes, glucose level, and risk of sudden cardiac death. Eur Heart J 26:2142–2147. 10.1093/eurheartj/ehi376 [PubMed: 15980034]

19. Jovanovic S, Jovanovic A (2005) High glucose regulates the activity of cardiac sarcolemmal ATP-sensitive K+ channels via 1,3-bisphosphoglycerate: a novel link between cardiac membrane excitability and glucose metabolism. Diabetes 54:383–393. 10.2337/diabetes.54.2.383 [PubMed: 15677496]

20. King AJ (2012) The use of animal models in diabetes research. Br J Pharmacol 166:877–894. 10.1111/j.1476-5381.2012.01911.x [PubMed: 22352879]

21. Kronlage M, Dewenter M, Grosso J, Fleming T, Oehl U, Lehmann LH, Falcao-Pires I, Leite-Moreira AF, Volk N, Grone HJ, Muller OJ, Sickmann A, Katus HA, Backs J (2019) O-GlcNAcylation of histone deacetylase 4 protects the diabetic heart from failure. Circulation 140:580–594. 10.1161/CIRCULATIONAHA.117.031942 [PubMed: 31195810]

22. Lengyel C, Virag L, Biro T, Jost N, Magyar J, Biliczki P, Kocsis E, Skoumal R, Nanasi PP, Toth M, Kecskemeti V, Papp JG, Varro A (2007) Diabetes mellitus attenuates the repolarization reserve in mammalian heart. Cardiovasc Res 73:512–520. 10.1016/j.cardiores.2006.11.010 [PubMed: 17182020]

23. Ling H, Zhang T, Pereira L, Means CK, Cheng H, Gu Y, Dalton ND, Peterson KL, Chen J, Bers D, Brown JH (2009) Requirement for Ca^{2+}/calmodulin-dependent kinase II in the transition from pressure overload-induced cardiac hypertrophy to heart failure in mice. J Clin Invest 119:1230–1240. 10.1172/JCI38022 [PubMed: 19381018]

24. Lu S, Liao Z, Lu X, Katschinski DM, Mercola M, Chen J, Heller Brown J, Molkentin JD, Bossuyt J, Bers DM (2020) Hyperglycemia acutely increases cytosolic reactive oxygen species via O-

linked glcnacylation and camkii activation in mouse ventricular myocytes. Circ Res 126:e80–e96. 10.1161/CIRCRESAHA.119.316288 [PubMed: 32134364]

25. Luo M, Guan X, Luczak ED, Lang D, Kutschke W, Gao Z, Yang J, Glynn P, Sossalla S, Swaminathan PD, Weiss RM, Yang B, Rokita AG, Maier LS, Efimov IR, Hund TJ, Anderson ME (2013) Diabetes increases mortality after myocardial infarction by oxidizing CaMKII. J Clin Invest 123:1262–1274. 10.1172/JCI65268 [PubMed: 23426181]

26. Ma J, Hart GW (2013) Protein O-GlcNAcylation in diabetes and diabetic complications. Expert Rev Proteomics 10:365–380. 10.1586/14789450.2013.820536 [PubMed: 23992419]

27. Magyar J, Rusznak Z, Szentesi P, Szucs G, Kovacs L (1992) Action potentials and potassium currents in rat ventricular muscle during experimental diabetes. J Mol Cell Cardiol 24:841–853. 10.1016/0022-2828(92)91098-p [PubMed: 1433314]

28. Marfella R, Nappo F, De Angelis L, Siniscalchi M, Rossi F, Giugliano D (2000) The effect of acute hyperglycaemia on QTc duration in healthy man. Diabetologia 43:571–575. 10.1007/s001250051345 [PubMed: 10855531]

29. Meo M, Meste O, Signore S, Sorrentino A, Cannata A, Zhou Y, Matsuda A, Luciani M, Kannappan R, Goichberg P, Leri A, Anversa P, Rota M (2016) Reduction in Kv current enhances the temporal dispersion of the action potential in diabetic myocytes: insights from a novel repolarization algorithm. J Am Heart Assoc. 10.1161/JAHA.115.003078

30. Nakamura TY, Coetzee WA, Vega-Saenz De Miera E, Artman M, Rudy B (1997) Modulation of Kv4 channels, key components of rat ventricular transient outward K^+ current, by PKC. Am J Physiol 273:H1775–1786. 10.1152/ajpheart.1997.273.4.H1775 [PubMed: 9362243]

31. Nishio S, Teshima Y, Takahashi N, Thuc LC, Saito S, Fukui A, Kume O, Fukunaga N, Hara M, Nakagawa M, Saikawa T (2012) Activation of CaMKII as a key regulator of reactive oxygen species production in diabetic rat heart. J Mol Cell Cardiol 52:1103–1111. 10.1016/j.yjmcc.2012.02.006 [PubMed: 22394624]

32. Nystoriak MA, Nieves-Cintron M, Nygren PJ, Hinke SA, Nichols CB, Chen CY, Puglisi JL, Izu LT, Bers DM, Dell'acqua ML, Scott JD, Santana LF, Navedo MF (2014) AKAP150 contributes to enhanced vascular tone by facilitating large-conductance Ca^{2+}-activated K^+ channel remodeling in hyperglycemia and diabetes mellitus. Circ Res 114:607–615. 10.1161/CIRCRESAHA.114.302168 [PubMed: 24323672]

33. Po SS, Wu RC, Juang GJ, Kong W, Tomaselli GF (2001) Mechanism of alpha-adrenergic regulation of expressed hKv4.3 currents. Am J Physiol Heart Circ Physiol 281:H2518–2527. 10.1152/ajpheart.2001.281.6.H2518 [PubMed: 11709419]

34. Pogwizd SM, Schlotthauer K, Li L, Yuan W, Bers DM (2001) Arrhythmogenesis and contractile dysfunction in heart failure: Roles of sodium-calcium exchange, inward rectifier potassium current, and residual beta-adrenergic responsiveness. Circ Res 88:1159–1167. 10.1161/hh1101.091193 [PubMed: 11397782]

35. Polina I, Jansen HJ, Li T, Moghtadaei M, Bohne LJ, Liu Y, Krishnaswamy P, Egom EE, Belke DD, Rafferty SA, Ezeani M, Gillis AM, Rose RA (2020) Loss of insulin signaling may contribute to atrial fibrillation and atrial electrical remodeling in type 1 diabetes. Proc Natl Acad Sci U S A 117:7990–8000. 10.1073/pnas.1914853117 [PubMed: 32198206]

36. Ravens U, Cerbai E (2008) Role of potassium currents in cardiac arrhythmias. Europace 10:1133–1137. 10.1093/europace/eun193 [PubMed: 18653669]

37. Robles-Flores M, Melendez L, Garcia W, Mendoza-Hernandez G, Lam TT, Castaneda-Patlan C, Gonzalez-Aguilar H (2008) Posttranslational modifications on protein kinase c isozymes. Effects of epinephrine and phorbol esters. Biochim Biophys Acta 1783:695–712. 10.1016/j.bbamcr.2007.07.011 [PubMed: 18295358]

38. Roeper J, Lorra C, Pongs O (1997) Frequency-dependent inactivation of mammalian A-type K^+ channel KV1.4 regulated by Ca^{2+}/calmodulin-dependent protein kinase. J Neurosci 17:3379–3391 [PubMed: 9133364]

39. Sato T, Kobayashi T, Kuno A, Miki T, Tanno M, Kouzu H, Itoh T, Ishikawa S, Kojima T, Miura T, Tohse N (2014) Type 2 diabetes induces subendocardium-predominant reduction in transient outward K^+ current with downregulation of Kv4.2 and KChIP2. Am J Physiol Heart Circ Physiol 306:H1054–1065. 10.1152/ajpheart.00414.2013 [PubMed: 24486512]

40. Schmitt N, Grunnet M, Olesen SP (2014) Cardiac potassium channel subtypes: new roles in repolarization and arrhythmia. Physiol Rev 94:609–653. 10.1152/physrev.00022.2013 [PubMed: 24692356]

41. Sergeant GP, Ohya S, Reihill JA, Perrino BA, Amberg GC, Imaizumi Y, Horowitz B, Sanders KM, Koh SD (2005) Regulation of Kv4.3 currents by Ca^{2+}/calmodulin-dependent protein kinase II. Am J Physiol Cell Physiol 288:C304–313. 10.1152/ajpcell.00293.2004 [PubMed: 15456698]

42. Slot JW, Geuze HJ, Gigengack S, James DE, Lienhard GE (1991) Translocation of the glucose transporter GLUT4 in cardiac myocytes of the rat. Proc Natl Acad Sci U S A 88:7815–7819. 10.1073/pnas.88.17.7815 [PubMed: 1881917]

43. Syed AU, Reddy GR, Ghosh D, Prada MP, Nystoriak MA, Morotti S, Grandi E, Sirish P, Chiamvimonvat N, Hell JW, Santana LF, Xiang YK, Nieves-Cintron M, Navedo MF (2019) Adenylyl cyclase 5-generated cAMP controls cerebral vascular reactivity during diabetic hyperglycemia. J Clin Invest 129:3140–3152. 10.1172/JCI124705 [PubMed: 31162142]

44. Tenma T, Mitsuyama H, Watanabe M, Kakutani N, Otsuka Y, Mizukami K, Kamada R, Takahashi M, Takada S, Sabe H, Tsut-sui H, Yokoshiki H (2018) Small-conductance Ca^{2+}-activated K^+ channel activation deteriorates hypoxic ventricular arrhythmias via CaMKII in cardiac hypertrophy. Am J Physiol Heart Circ Physiol 315:H262–H272. 10.1152/ajpheart.00636.2017 [PubMed: 29631373]

45. Thomas D, Zhang W, Wu K, Wimmer AB, Gut B, Wendt-Nordahl G, Kathofer S, Kreye VA, Katus HA, Schoels W, Kiehn J, Karle CA (2003) Regulation of HERG potassium channel activation by protein kinase C independent of direct phosphorylation of the channel protein. Cardiovasc Res 59:14–26. 10.1016/s0008-6363(03)00386-9 [PubMed: 12829172]

46. Tran HV, Gore JM, Darling CE, Ash AS, Kiefe CI, Goldberg RJ (2018) Hyperglycemia and risk of ventricular tachycardia among patients hospitalized with acute myocardial infarction. Cardiovasc Diabetol 17:136. 10.1186/s12933-018-0779-8 [PubMed: 30340589]

47. Vega RB, Harrison BC, Meadows E, Roberts CR, Papst PJ, Olson EN, McKinsey TA (2004) Protein kinases C and D mediate agonist-dependent cardiac hypertrophy through nuclear export of histone deacetylase 5. Mol Cell Biol 24:8374–8385. 10.1128/MCB.24.19.8374-8385.2004 [PubMed: 15367659]

48. Wagner S, Hacker E, Grandi E, Weber SL, Dybkova N, Sossalla S, Sowa T, Fabritz L, Kirchhof P, Bers DM, Maier LS (2009) Ca/calmodulin kinase II differentially modulates potassium currents. Circ Arrhythm Electrophysiol 2:285–294. 10.1161/CIRCEP.108.842799 [PubMed: 19808479]

49. Wu X, Zhang T, Bossuyt J, Li X, McKinsey TA, Dedman JR, Olson EN, Chen J, Brown JH, Bers DM (2006) Local InsP3-dependent perinuclear Ca^{2+} signaling in cardiac myocyte excitation-transcription coupling. J Clin Invest 116:675–682. 10.1172/JCI27374 [PubMed: 16511602]

50. Xu H, Guo W, Nerbonne JM (1999) Four kinetically distinct depolarization-activated K^+ currents in adult mouse ventricular myocytes. J Gen Physiol 113:661–678. 10.1085/jgp.113.5.661 [PubMed: 10228181]

51. Xu Z, Patel KP, Lou MF, Rozanski GJ (2002) Up-regulation of K(+) channels in diabetic rat ventricular myocytes by insulin and glutathione. Cardiovasc Res 53:80–88. 10.1016/s0008-6363(01)00446-1 [PubMed: 11744015]

52. Zhang DM, Chai Y, Erickson JR, Brown JH, Bers DM, Lin YF (2014) Intracellular signalling mechanism responsible for modulation of sarcolemmal ATP-sensitive potassium channels by nitric oxide in ventricular cardiomyocytes. J Physiol 592:971–990. 10.1113/jphysiol.2013.264697 [PubMed: 24277866]

53. Zhang T, Maier LS, Dalton ND, Miyamoto S, Ross J Jr, Bers DM, Brown JH (2003) The deltaC isoform of CaMKII is activated in cardiac hypertrophy and induces dilated cardiomyopathy and heart failure. Circ Res 92:912–919. 10.1161/01.RES.0000069686.31472.C5 [PubMed: 12676814]

54. Zhang Y, Xiao J, Lin H, Luo X, Wang H, Bai Y, Wang J, Zhang H, Yang B, Wang Z (2007) Ionic mechanisms underlying abnormal QT prolongation and the associated arrhythmias in diabetic rabbits: a role of rapid delayed rectifier K^+ current. Cell Physiol Biochem 19:225–238. 10.1159/000100642 [PubMed: 17495463]
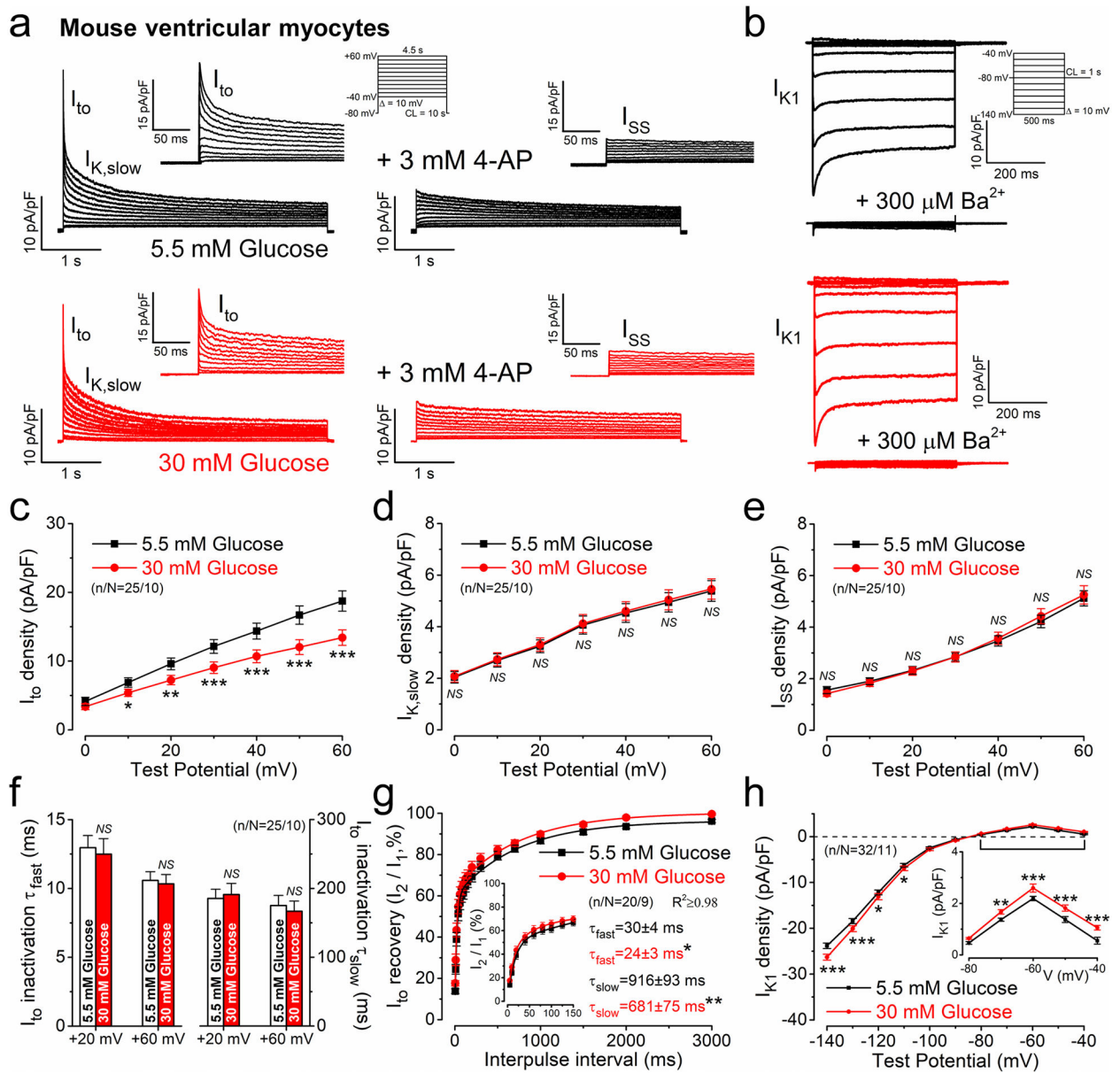
Fig. 1.

Acute hyperglycemia regulates K^+ channels in mouse ventricular cardiomyocytes. **a** Representative voltage-gated K^+ current traces in normoglycemia and acute hyperglycemia. The transient outward K^+ current (I_{to}) and slowly-inactivating K^+ current ($I_{K,slow}$) were inhibited by 3 mmol/L 4-aminopyiridine. Inset shows enlarged I_{to}. The steady-state K^+ current (I_{SS}) was insensitive to 4-aminopyridine. **b** Representative inward rectifier K^+ current (I_{K1}) traces. **c** I_{to} was significantly reduced in acute hyperglycemia. **d, e** $I_{K,slow}$ and I_{SS} were unaltered in acute hyperglycemia. **f** I_{to} fast and slow inactivation time constants (τ_{fast} and τ_{slow}) were unchanged in acute hyperglycemia. **g** I_{to} recovery from inactivation was faster in hyperglycemia. **h** I_{K1} increased in acute hyperglycemia. Student's paired *t* test, $*p < 0.05$, $**p < 0.01$, $***p < 0.001$
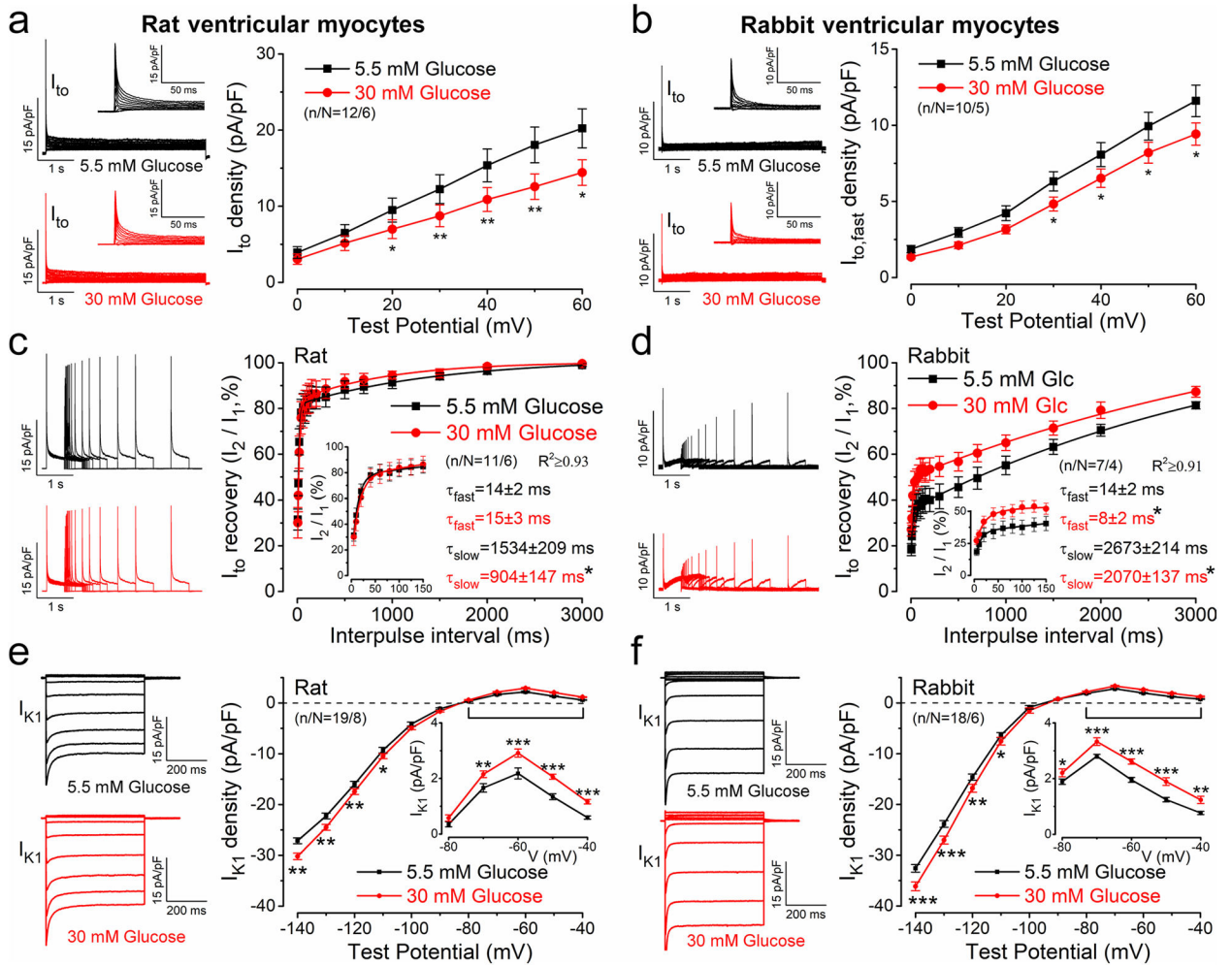
Fig. 2.
Acute hyperglycemia regulates K^+ currents in rat and rabbit ventricular myocytes. **a**, **b** Representative I_{to} traces and averaged data in normoglycemia and hyperglycemia conditions in rat (**a**) and rabbit (**b**) ventricular myocytes. **c**, **d** Enhanced I_{to} recovery from inactivation kinetics in hyperglycemia in both rat (**c**) and rabbit (**d**) cardiomyocytes. **e**, **f** Representative I_{K1} traces and averaged data in rat (**e**) and rabbit (**f**). Student's paired *t* test; *$p < 0.05$, **$p < 0.01$, ***$p < 0.001$
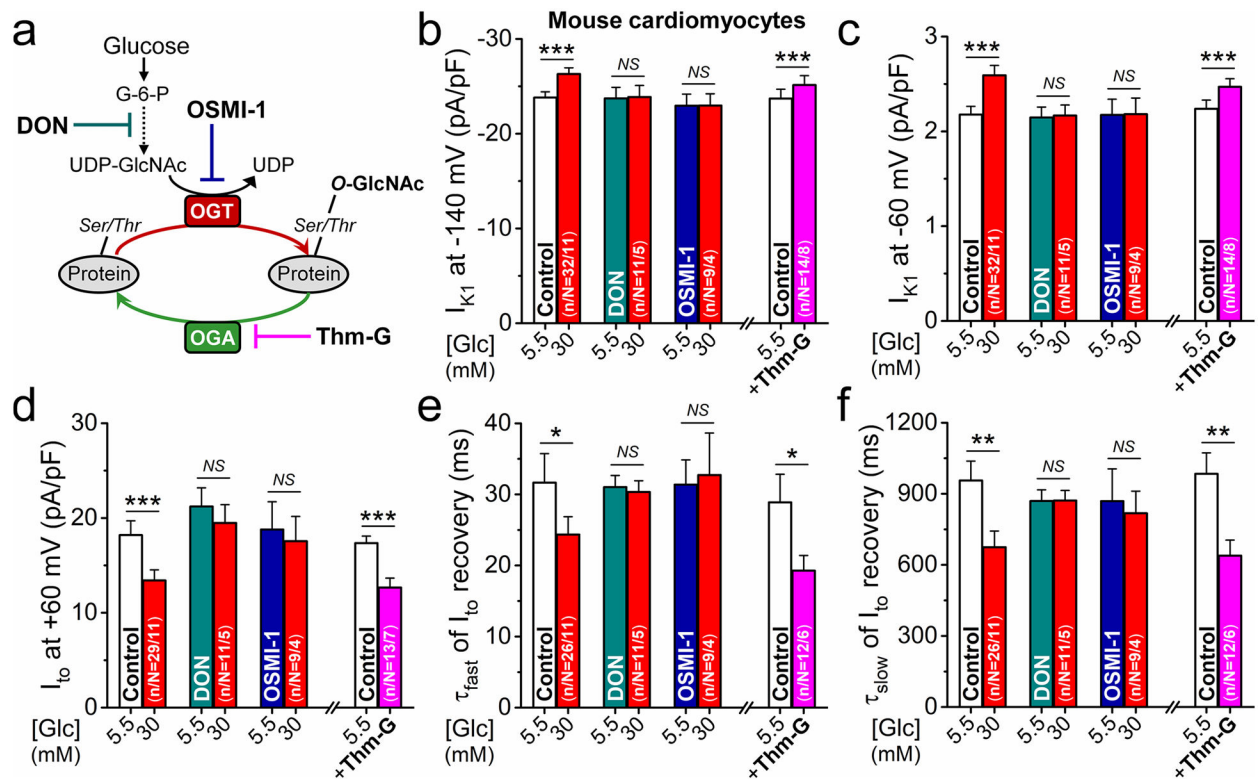
Fig. 3.

O-GlcNAc pathway mediates the K$^+$ channel effects in hyperglycemia. **a** Schematic of *O*-GlcNAc modifications and targets for pharmacological interventions. **b–f** Inhibition of *O*-GlcNAc pathway using 6-diazo-5-oxo-L-norleucine (DON, 50 μmol/L) or the specific *O*-GlcNAc transferase (OGT) inhibitor OSMI-1 (50 μmol/L) prevented hyperglycemia-induced changes both in I$_{K1}$ density (**b**, **c**), I$_{to}$ density (**d**), and I$_{to}$ recovery kinetics (**e**, **f**) in mouse ventricular myocytes. Conversely, inhibiting the *O*-GlcNAc removal enzyme (O-Glc-NAc*ase*, OGA) using Thiamet-G (Thm-G, 100 nmol/L) promoted glucose effects on K$^+$ currents already in normoglycemia. Student's paired *t* test; *$p < 0.05$, **$p < 0.01$, ***$p < 0.001$
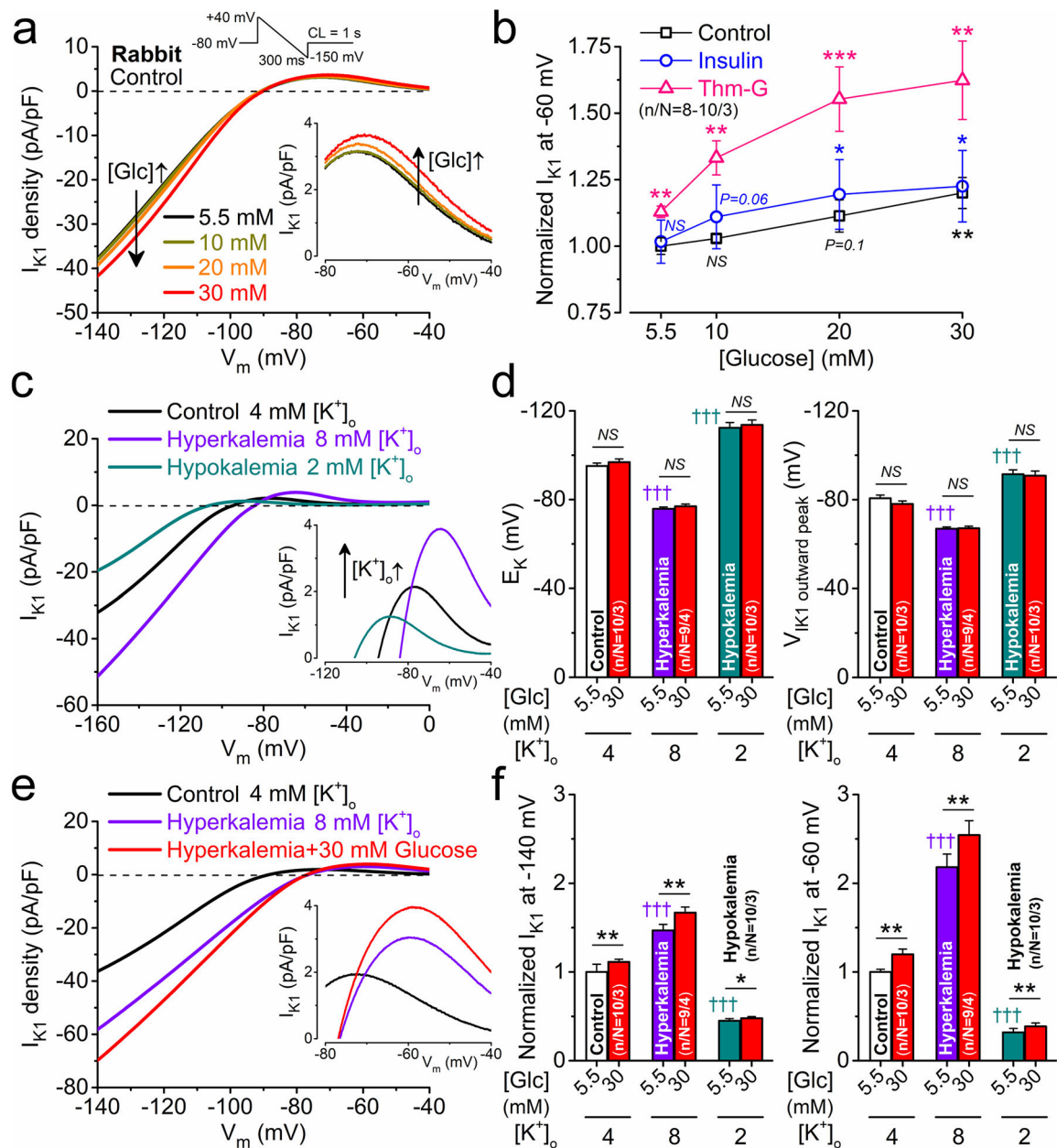
Fig. 4.

Glucose dose-response on I_{K1} and effect of changing extracellular K^+ concentration. **a** Representative I_{K1} traces measured using a ramp protocol (shown above) in the presence of increasing concentrations of glucose in rabbit ventricular myocytes. **b** Glucose dose–response curves on I_{K1} at -60 mV in control and following pretreatments with either insulin (5 nmol/L) or Thiamet-G (Thm-G, 100 nmol/L). **c** Representative I_{K1} traces in hyperkalemia and hypokalemia. **d** Hyperkalemia and hypokalemia shifted the reversal potential of I_{K1} (E_K) and the voltage, where outward I_{K1} peaked. **e** Representative I_{K1} traces in combined hyperkalemia and hyperglycemia. **f** Hyperglycemia markedly increased I_{K1} in hyperkalemia and slightly increased in hypokalemia. Two-way ANOVA; $*p < 0.05$, $**p < 0.01$, $***p < 0.001$ vs. normoglycemia; $^{†††}p < 0.001$ vs. control
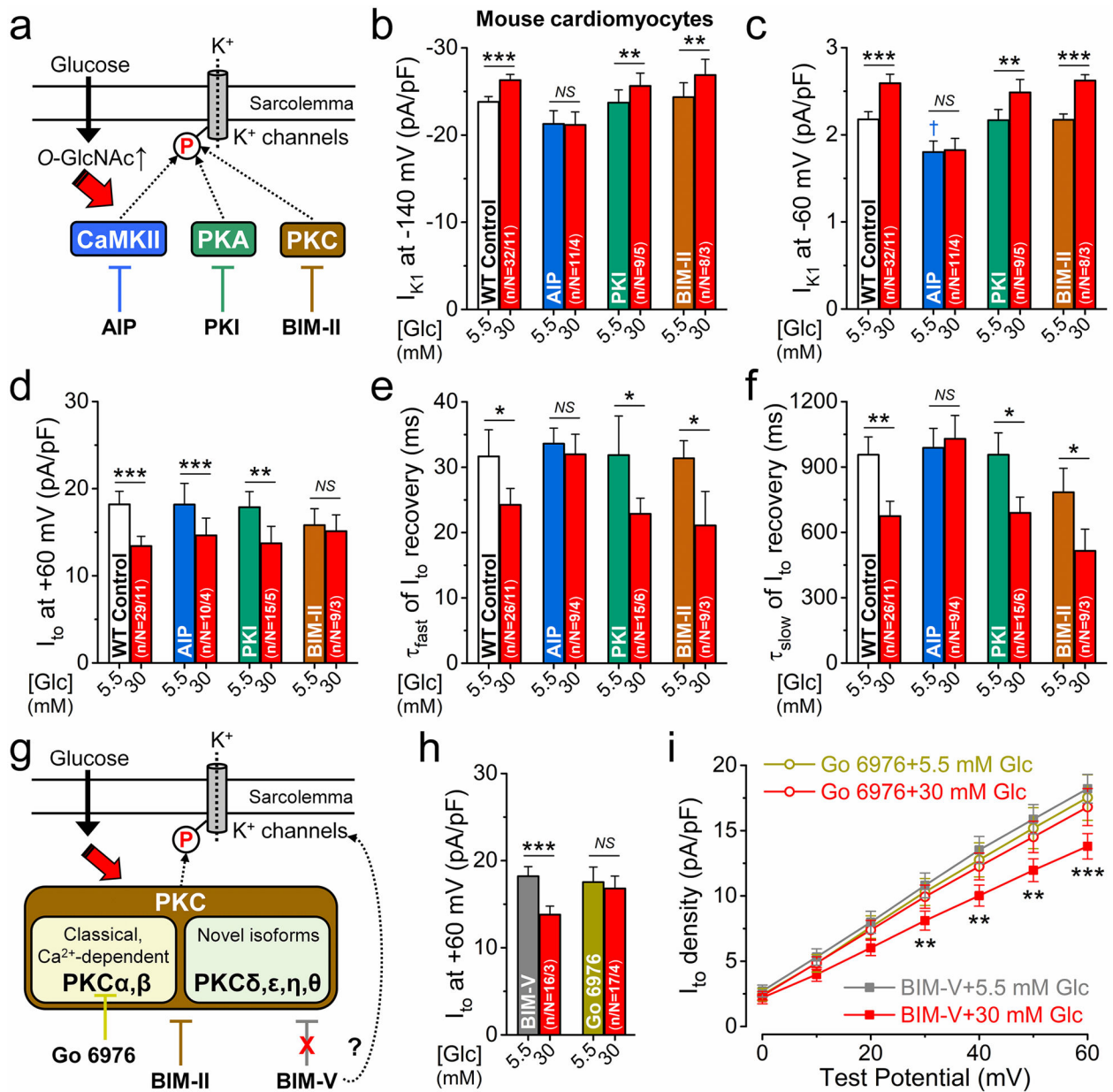
Fig. 5.

CaMKII and PKC mediate the hyperglycemia effects on K^+ channels. **a** Schematic of potential protein kinase pathways that may mediate the hyperglycemia effects on K^+ channels and their selective inhibitors. **b**–**f** Inhibition of CaMKII using the specific autocamp-tide-2 related inhibitory peptide (AIP, 1 μmol/L) prevented the hyperglycemia effects on I_{K1} (**b**, **c**) and I_{to} recovery (**e**, **f**) in mouse ventricular myocytes. Selective inhibition of protein kinase C (PKC) using bisindolylmaleimide II (BIM-II, 100 nmol/L) prevented I_{to} reduction in hyperglycemia (**d**). Protein kinase A (PKA) inhibition using the selective protein kinase inhibitory peptide (PKI, 1 μmol/L) had no effect on K^+ channels in hyperglycemia. **g** Schematic of PKC isoforms and inhibitors. **h** Go 6976 (100 nmol/L), a selective inhibitor of conventional, Ca^{2+}-dependent PKC isoforms (PKCα and β) prevented

I_{to} reduction in hyperglycemia. BIM-V (100 nmol/L), a structurally related but inactive analogue of PKC inhibitors had no effect on I_{to} in normal glucose and did not prevent I_{to} reduction in hyperglycemia. **i** I-V relationship of I_{to} following Go 6976 and BIM-V pretreatments. Two-way ANOVA; $*p < 0.05$, $**p < 0.01$, $***p < 0.001$ vs. normoglycemia; $^{\dagger}p < 0.05$ vs. control
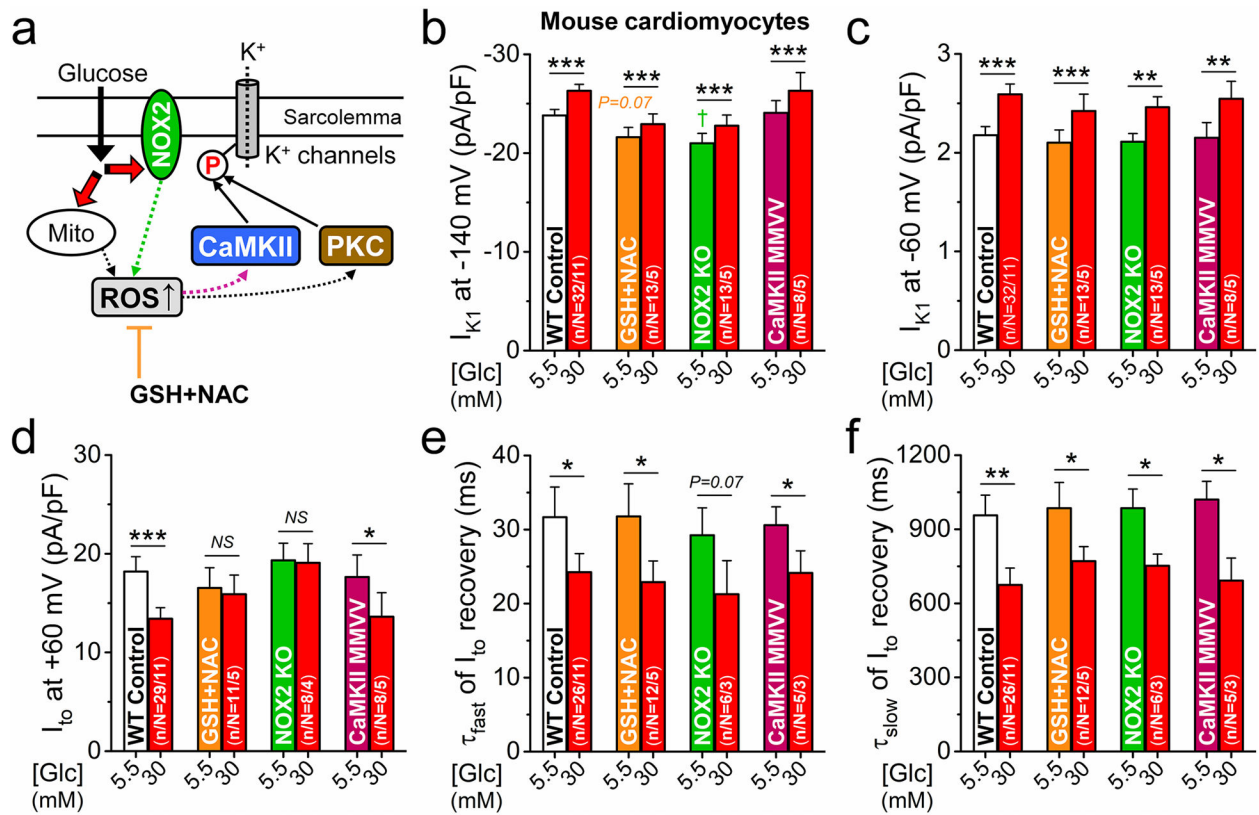
Fig. 6.

NOX2-dependent ROS production mediates I_{to} reduction in hyperglycemia. **a** Schematic signaling via reactive oxygen species (ROS) that may be involved in the hyperglycemia effects on K^+ channels. **b**–**f** Pretreatment of mouse ventricular myocytes with ROS scavengers, reduced glutathione (GSH, 10 mmol/L) and *N*-acetylcysteine (NAC, 10 mmol/L), prevented I_{to} downregulation (**d**) but not I_{K1} (**b**, **c**) and I_{to} recovery (**e**, **f**) effects in hyperglycemia. I_{to} in NADPH oxidase 2 (NOX2)-knockout was also resistant to acute hyperglycemia. Oxidation-resistant CaMKIIδ-MMVV knock-in was not protected against acute hyperglycemia effects on either I_{K1} or I_{to}. Two-way ANOVA; *$p < 0.05$, **$p < 0.01$, ***$p < 0.001$ vs. normoglycemia; †$p < 0.05$ vs. control
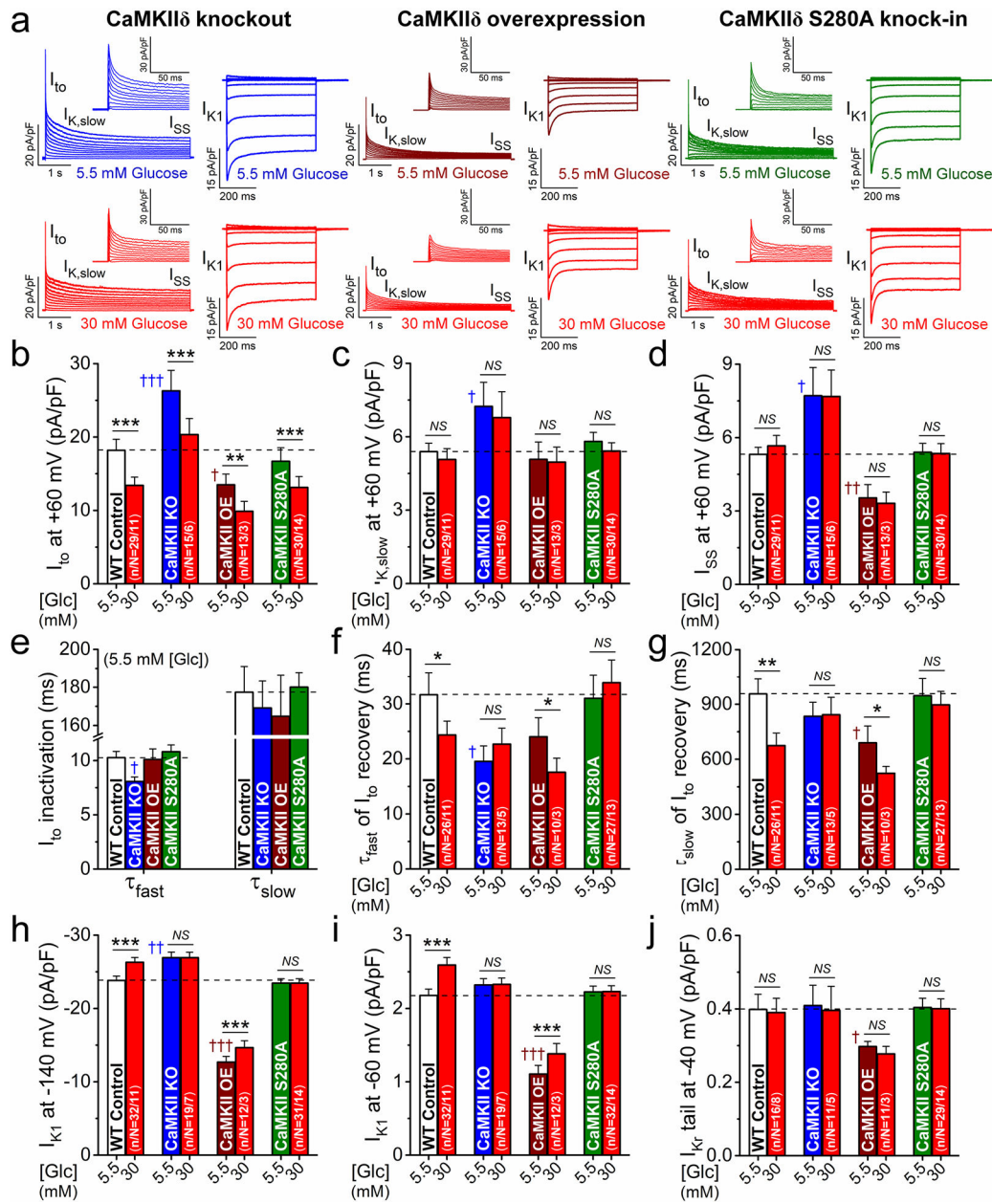
Fig. 7.

CaMKII activation via S280 *O*-GlcNAcylation regulates I_{K1} and I_{to} recovery in hyperglycemia. **a** Representative voltage-gated K⁺ currents and I_{K1} traces in normoglycemia and hyperglycemia in CaMKIIδ-knockout (KO), overexpression (OE) and *O*-GlcNAc-resistant S280A knock-in mouse myocytes. **b–j** K⁺ current remodeling in CaMKIIδ-KO and OE in normoglycemia. CaMKIIδ-S280A had a normal baseline phenotype. Hyperglycemia effects on I_{to} recovery kinetics (**f, g**) and I_{K1} (**h, i**) but not on I_{to} amplitude (**b**) were prevented in both CaMKIIδ-KO and S280A. Two-way ANOVA; *$p < 0.05$, **$p < 0.01$, ***$p < 0.001$ vs. normoglycemia; †$p < 0.05$, ††$p < 0.01$, †††$p < 0.001$ vs. WT control
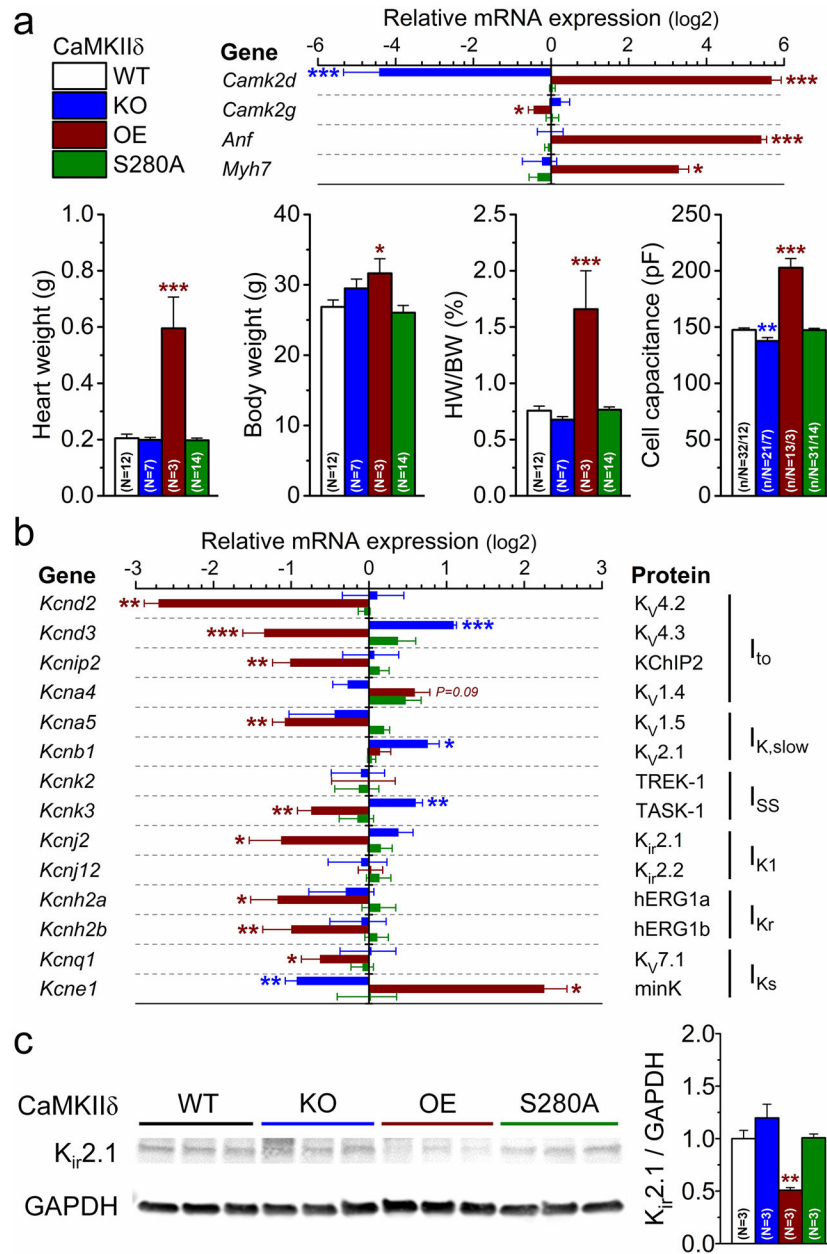
Fig. 8.
CaMKII regulates cardiac hypertrophy and K^+ channel expression. **a** qRT-PCR data on expression of Camk2d, Camk2g, and hypertrophic genes (Anf, Myh7) and morphometric parameters in CaMKIIδ-knockout (KO), overexpression (OE) and *O*-GlcNAc-resistant S280A knock-in mouse hearts. **b** mRNA expression of K^+ channel genes normalized to WT control. **c** Western blot analysis of $K_{ir}2.1$ expression normalized to WT control. ANOVA; *$p < 0.05$, **$p < 0.01$, ***$p < 0.001$
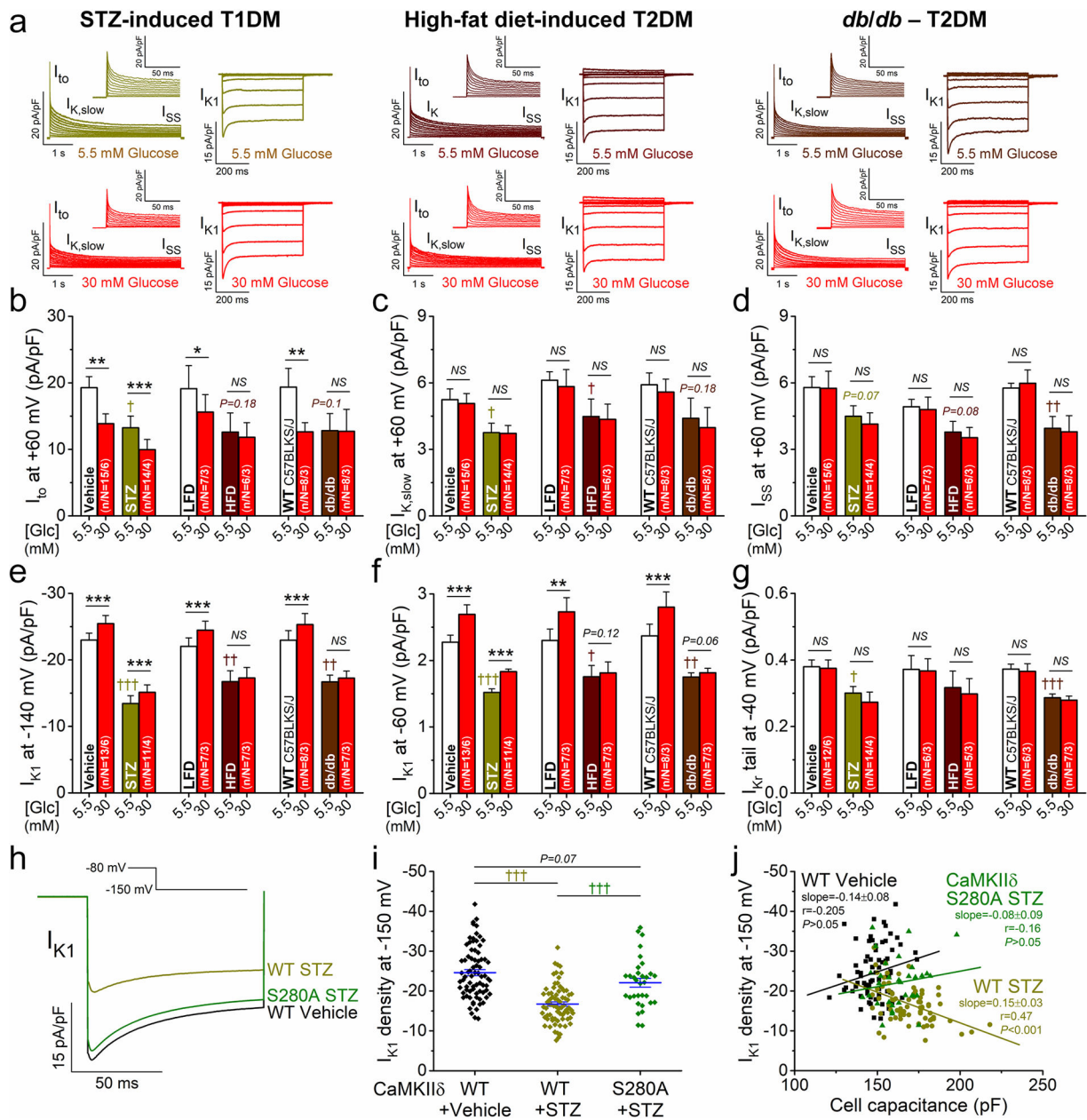
Fig. 9.
Diabetes induces remodeling in K$^+$ currents in mouse ventricular myocytes. **a** Representative voltage-gated K$^+$ currents and I$_{K1}$ traces in normoglycemia and hyperglycemia in streptozotocin (STZ)-induced T1DM, high-fat diet (HFD)-induced T2DM, and *db/db* mouse myocytes. **b**–**g** Decreases of K$^+$ currents in DM vs. corresponding controls: vehicle-injection for STZ, low-fat diet (LFD) for HFD and C57BLKS/J for db/db. Hyperglycemia further reduced I$_{to}$ and increased I$_{K1}$ in STZ (and all controls), but not in HFD and db/db. **h** Representative I$_{K1}$ traces measured at – 150 mV in STZ-treated WT, *O*-GlcNAc-resistant CaMKIIδ-S280A knock-in, and vehicle-treated WT control. **i** The decrease in I$_{K1}$ density was markedly attenuated in STZ-treated CaMKIIδ-S280A. **j** The cell capacitance correlated with the decrease in I$_{K1}$ density in STZ-treated WT, whereas no

correlation was found in WT control and STZ-treated CaMKIIδ-S280A. Lines indicate linear regression. Two-way ANOVA; *$p < 0.05$, **$p < 0.01$, ***$p < 0.001$ vs. normoglycemia; †$p < 0.05$, ††$p < 0.01$, †††$p < 0.001$ vs. control
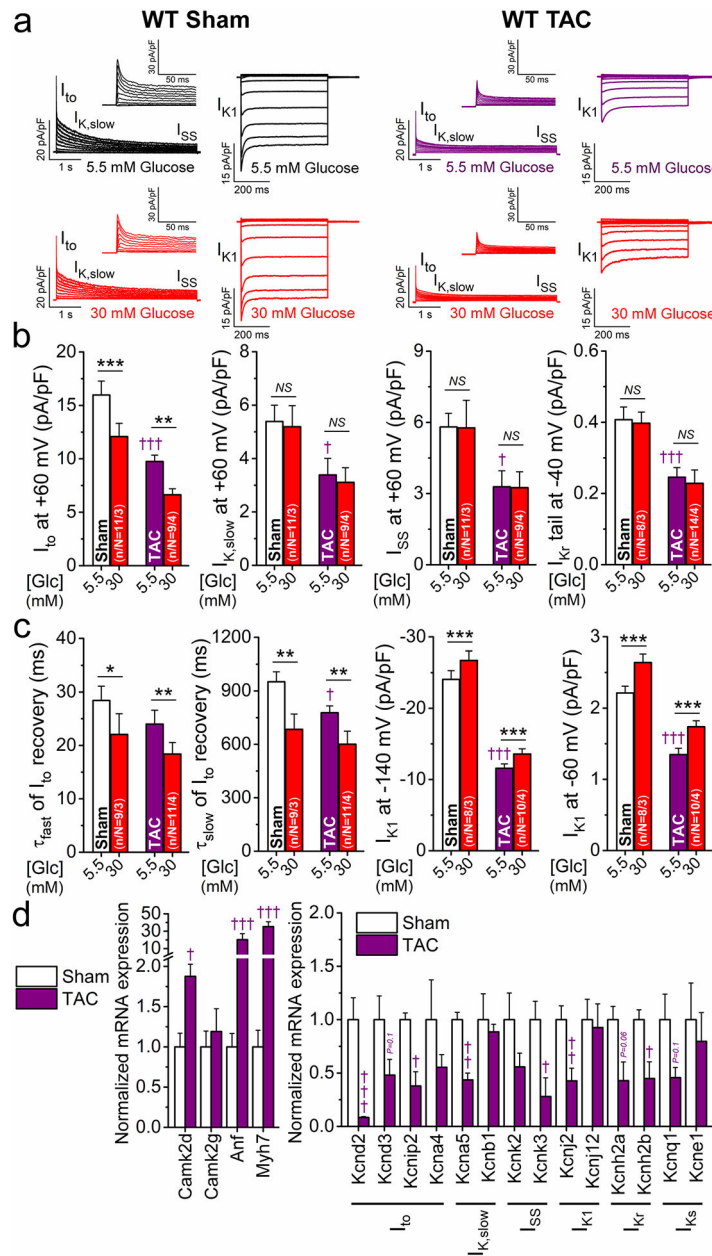
Fig. 10.
K$^+$ channel remodeling and hyperglycemia effects in heart failure. **a** Representative voltage-gated K$^+$ currents and I$_{K1}$ traces in normoglycemia and hyperglycemia in transverse aortic constriction (TAC)-induced heart failure (8-week post-TAC) vs. sham mouse myocytes. **b** K$^+$ current remodeling in TAC. Hyperglycemia further reduced I$_{to}$ in TAC. **c** Hyperglycemia slightly enhanced I$_{to}$ recovery kinetics and increased the markedly downregulated I$_{K1}$ in TAC. **d** Normalized qRT-PCR data on expression of Camk2d and Camk2g, hypertrophic markers (Anf, Myh7) and K$^+$ channel genes. ANOVA; *$p < 0.05$. **$p < 0.01$, ***$p < 0.001$ vs. normoglycemia; †$p < 0.05$, ††$p < 0.01$, †††$p < 0.001$ vs. sham